Heat Mass Transfer (2011) 47:519–540
DOI 10.1007/s00231-010-0742-z

ORIGINAL

Laser nitriding: investigations on the model system TiN. A review

Daniel Höche · Peter Schaaf

Received: 25 August 2009 / Accepted: 25 November 2010 / Published online: 15 December 2010
© Springer-Verlag 2010

Abstract Nitriding is a well known technique to improve properties of materials. The process utilizing laser contains many different processes like heat transport and melting effects, diffusion and convection, which partially determine the synthesized coatings. This review concludes the research on titanium nitride synthesis in reactive ambient and draws conclusions for the general handling of the method. Afterwards, it becomes clear which and why, transport processes limit the coating properties.

1 Introduction

Hard material systems such as titanium nitride play an important role within the field of material sciences and industrial applications. In particular wear and corrosion protection are based on such systems. Beside the classical manufacturing procedures such as PVD or CVD, the method of the direct laser synthesis in a reactive gas environment, as examined here, represents an alternative to the production of such coatings. This review discusses the synthesis of such functional coatings on the system titanium–nitrogen by different laser irradiation based on own results, respectively the literature and tries to give a general overview of the physical, respectively, transport processes taking place. Thus, experiments from the last three decades using similar experimental setups will be compared and discussed. Due to the availability of data of investigations utilizing titanium and nitrogen, this system was taken as a general model. After a discussion of several different experimental analyses and modelling results, the treatments get parameterized. This results in large potentials for technical applications. Finally, general conditions for the synthesis of such coatings with this procedure were set up. By means of these results it is possible to achieve purposefully predefined layer characteristics. The review concludes the most important publications containing research about this process. Thus, it could be assumed to be a reference in relation to laser nitriding or -carburizing.

1.1 Scope

Surface treatment of strained materials plays an important role in many parts of the research and the industry. Custom-made characteristics are produced by complex procedures. Thus, coatings or structures are manufactured, which possess optimized properties and characteristics in relation to, for example, optics or fluid mechanics. Typical applications for wear- and corrosion resistance are hard material coatings like TiN, AlN, TiCN, c-BN, Si_3N_4, which bear up extreme mechanical or thermal stresses. The production of such protective coatings takes place by means of well-known procedures like reactive sputtering from the wide field of the physical vapour deposition (PVD) [1], the chemical vapour deposition (CVD) [2], epitaxial procedures like the molecular beam epitaxy (MBE) [3], the pulsed laser deposition (PLD) [4] or also hybrid

D. Höche (✉)
Helmholtz-Zentrum Geesthacht Zentrum für Material- und Küstenforschung GmbH, Institute of Materials Research, Max-Planck-Straße 1, 21502 Geesthacht, Germany
e-mail: Daniel.Hoeche@hzg.de

D. Höche
II. Physikalisches Institut, Universität Göttingen, Friedrich Hund Platz 1, 37077 Göttingen, Germany

P. Schaaf
TU Ilmenau, Institut für Werkstofftechnik, FG Werkstoffe der Elektrotechnik, 98684 Ilmenau, Germany

procedures. A further alternative and very simple method is the direct lasers synthesis. The material is placed in a reactive gas environment and will be irradiated with laser light. Due to the developing physical and chemical effects coatings are synthesized, which possess special treatment dependent characteristics. Carburizing, nitro carburizing and/or nitriding are the most common methods from this field of processes. The method of nitriding particularly assists the improvement of tribological properties of surfaces. The surface hardness gets increased, whereby the wear resistance rises. Furthermore, these coatings are usually very non-reactive, which leads to an increase in corrosion protection.

In the following the method will be studied more exactly and will be explained. Quantifying of the processes gets an important aim of the work. Arising phenomena will also be modelled. To do these investigations, the model titanium nitrogen has been used. It is a well known and often used system, and has been investigated many times in the past. By bringing nitrogen into the titanium matrix it is possible to synthesize titanium nitride phases which possess special mechanical or also electrical characteristics. TiN is used frequently for the refinement of cutting or drilling tools. Besides, it is very often used due to its chemical characteristics with bio implants. Classical manufacturing processes are here in particular the plasma or gas nitriding. Pure titanium is sublimated, whereby it reacts with the available nitrogen.

1.2 Recent developments

As instructed, in many parts of the research and industry coatings are used, in order to achieve specific characteristics. In the DIN 8580 cladding is mentioned as a main group of the manufacturing methods and the individual techniques are assigned. An organization into four groups of the application fields can roughly be made. First, the classical mechanical applications are to be called here. Tribological characteristics are improved and thus the wear and corrosion protection are strengthened. In addition, hard material systems are produced, which are usually based on carbides or nitrides. These systems are besides high temperature-steadily. Since the pallet of suitable compositions is limited, lately one tried to develop new systems or to manufacture alloys with tailored microstructures. As a further group one can define coatings, which must satisfy special requirements. For example demands are made against the wettability, electrical and/or semi conducting characteristics which are needed in high-technological applications. Among this group also the large field of the optical coatings, which are used in eyeglasses or within the laser based technology, has to be named. The third group can be interpreted as coatings for special materials. Thus, in the biomedicine or particularly within the implants, compatible systems are used, which improve the compatibility and the durability. At least the group of decorative coating can be called.

The laser material processing held in many parts of the industry and is now a commercial tool hardly being excluded. In process technical point of view, hardening, alloying, welding, drilling and cutting are established methods [5–7]. The processes taking place during the laser irradiation, lead to the change of material properties, to different phases and to structural formations. For example purposeful welding seam characteristics can be reached. By means of high-energy laser systems welding into depths of some centimetres [8, 9] are possible. Using optical scanners it is possible to provide aperture masks with drilling geometries in high resolution. The listing here could be continued arbitrarily long. Regarding to surface treatments, hardening and alloying are the most common one.

The procedure examined here can be classified among the gas alloying. By inserting the energy into the material an environment is produced, which leads to an improved adhesion of atoms. The diffusion coefficient increases by orders of magnitude and the activity of the gas is increased too, which leads to an increase of the absorption rate. If the power density becomes very high, additionally remelting- and evaporation effects are arising. As a result of the ambient and the reacting effects, further new interesting aspects for the laser surface processing become important. This work will conclude all these aspects and will discuss the method in relation to industrial applications and will show, what is still to do.

2 Basics of laser nitriding

2.1 Literature

2.1.1 Laser treatments of titanium

The treatment of titanium or its alloys by means of laser light was frequently studied. On the one hand welding of titanium particularly in the light metal industry is well known, but also cladding techniques are established. For example Sun et al. [10] has used Ti6Al4V for cladding of tools. In an investigation of Yunlian et al. [11] the successful welding of titanium was shown. The behaviour of the titanium under irradiation of high-energy laser pulses has been studied by Basu et al. [12]. It is shown that with these high energies melt ejection develops, which based on the Piston-effect [13]. The evaporation behaviour of titanium during laser irradiation was investigated in [14] in every detail. Strong ablation behaviour and a strong feedback to the melt were observed. He et al. [15] structures

titanium surfaces by means of lasers on a microscopic level. Many further publications exist to this topic, thus it is unnecessary to give detailed executions. Regarding the procedure of the direct laser synthesis used here, however many interesting results can be transferred. For example from [16], where many properties of titanium melts have been investigated in relation to the treatment parameters. The method laser–gas alloying falls into the category described here.

2.1.2 Coating synthesis in reactive ambient

Coating synthesis in reactive atmospheres by means of lasers was examined in detail by Schaaf et al. [17] for different systems. Iron and silicon carbide in methane environments are synthesized, which significantly change the physical and chemical characteristics of the materials. Interesting experiments at silicon were accomplished in [18]. A very stable SiC phase was produced. In [19] essential characteristics of steel are changed by this method. Nitriding seems to be among them the most frequently used method. Thus, for example the very interesting iron nitrides in [20] were observed, which entails an enormous increase of the tribological properties. This is also observed for AlN in [21]. The most examined system for this method is probably TiN. For this reason it was selected for the investigations accomplished here. It allows a detailed insight into the process as well as their physics and the comparison of results of other researchers. As next, the work of several investigations on nitriding of titanium utilizing laser will be instructed.

2.1.3 Coating synthesis of TiN

The synthesis of TiN-coatings in reactive atmospheres by means of laser irradiation already goes back into the 80th and 90th of the last century [22–35]. They all show, that an enormous improvement of the properties of the materials is reached. For example in [36] characteristics of medical components such as implants are improved. Using CO_2 laser [37–39] coatings of some hundred micrometers thickness on different samples were realized, which led to an enormous increase of hardness. The experimental setup is relatively simple and resembles themselves at all publications. However, the processes taking place are very complex and will be discussed and compared in Sect. 2.4 more extensive. Still no uniform quantifying description exists. Nearly all investigations are based on post mortem principles, which lead to gaps in the understanding. The work of Labudovic et al. [40] and Nwobu et al. [41] tries to analyze the entire process more exactly. Labudovic indicates that the following reactions arise during the layer synthesis:

1. adsorption: $[\mathrm{Ti}] + \mathrm{N_2} \rightarrow [\mathrm{Ti}] + [\mathrm{N_2}]$
2. dissociation: $[\mathrm{N_2}] \rightarrow 2\mathrm{N}$
3. diffusion: $[\mathrm{N}](\mathrm{surface}) \rightarrow [\mathrm{N}](\mathrm{surface})$
4. TiN - formation: $[\mathrm{Ti(N)}] \rightarrow \mathrm{TiN} + [\mathrm{Ti(N)}]'$
5. solidification: $[\mathrm{Ti(N)}]' \rightarrow \mathrm{TiN} + \alpha - \mathrm{Ti(N)}$

Square brackets [] mean in liquid phase. This makes clear, which complex sequences going on during the process. It is shown that beside the TiN also nitrogen dissolution in the pure hexagonal α-titanium occurs. Nwobu discusses the problem similarly. He assumes the nitrogen is incorporated by convection into the liquid titanium and the melt reacts in an exothermal reaction. Various other authors for example in [42–48] have already studied the method utilizing diverse lasers and analysis methods. Most of their results will be discussed in relation to own investigations in Sect. 3. Afterwards some general conditions on laser nitriding will be postulated.

2.2 Experiments

For the execution of the experiments a relatively simple experimental setup was used. In recent publications [17, 18, 49–63] the preparation of the treatments was always the same. Setups from other authors were similar to that one and just vary in parameters and geometry. The untreated 1 mm thick titanium sheet metals (purity 99.98%) was cut in 15 × 15 mm^2 large pieces and was placed in a chamber, which has a quartz glass window on the top side. Afterwards the chamber was evacuated and finally filled with pure nitrogen (99.999 pct) on the corresponding pressure. The relative movement from laser beam to work piece was realized on an X–Y table or using an optical scanner. The experiment is represented in Fig. 1.

Since the aim of the method has the cladding of surfaces, the samples have been scanned in a meandering fashion. By variation of geometrical scan parameter, the energy and nitrogen incorporation has been controlled and offers the possibility to parameterize the process.

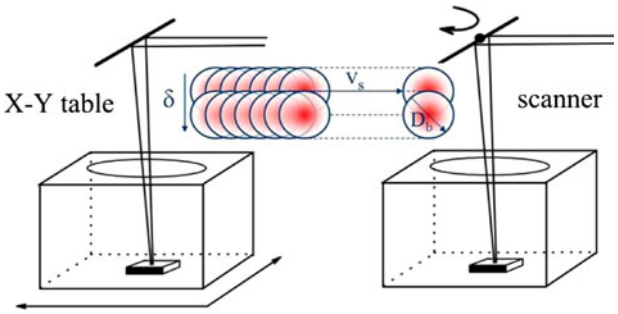

Fig. 1 Experimental setup for laser nitriding using a meandering fashion (δ, lateral shift; v_s, scan velocity; D_b, spot size)

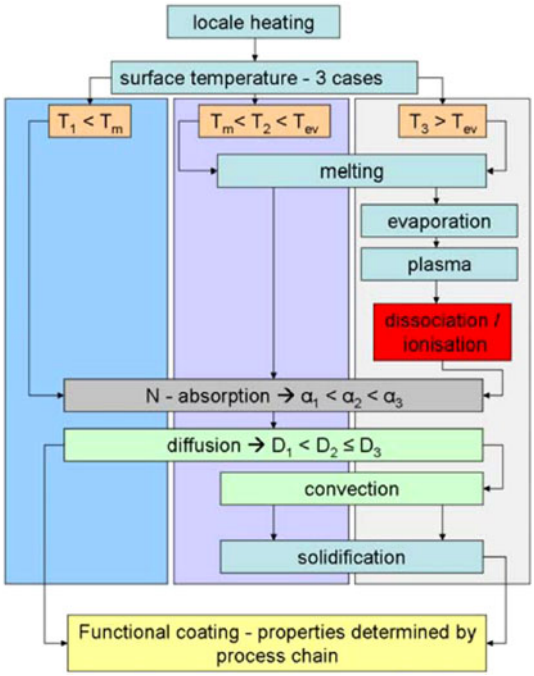

Fig. 2 Determination of different process chains depending on the surface temperature T_i—(T_m,melting point; T_{ev}, evaporation point; α_i, absorption coeff.; D_i, diffusion coeff.)

2.3 Process chains

Since the entire process is very complex and hard to describe, it is necessary to define and to quantify the individual physical and chemical sequences leading to different process chains. For this purpose a flow chart illustrated in Fig. 2 has been created, which helps to improve the understanding of processes taking place.

It shows the involved processes and the temporal operational sequence during the treatment. The entire process is dominated by the local heating and the resulting surface temperature. Depending on melting or evaporation effects, different process chains are involved. Finally, the coatings are determined by that one. It can be recognized, a process chain sets up itself, whereby each sub process causes consequences for the synthesis result. In order to improve the understanding, the aim of the investigation is to clarify and if necessary to quantify these influences. In relation to a complete description of the synthesis (technical application), investigations, measurements and simulations have to be compared and coupled. At the end appropriate conclusions should be pulled.

2.4 Physical processes and parameters

Contrary to the simple experimental setup for the direct laser synthesis, the physical and chemical mechanisms are very complex and in addition closely linked to each other. In order to understand and finally to control the treatments for applications in technology, the individual sub processes are examined. The following list shows the substantial ones:

- *Laser absorption and local heating:* First, the virgin material is irradiated, whereby a strong local heating takes place via optical absorption, which depends on the absorptivity resp. the optical characteristics (dielectric function), on the thermal conductivity and on the specific heat.
- *Melt and evaporation processes:* After reaching resp. exceeding the melting point and exceeding the latent heat of fusion a liquid phase develops, in which the material properties change rapidly. Here, in particular the improvement in the diffusion behaviour has to be considered. Besides, convection effects can arise, which affect the synthesis process especially the resulting surface quality significantly. A further energy entry leads to the excess of the evaporation threshold and results finally in ablation and plasma formation. All these processes depend on the energy density and the interaction time of the laser beam and are consistent to the three cases in the previous section.
- *Plasma expansion into the background gas:* Due to the pressure of the ambient gas the expansion gets strongly absorbed. The ratios of pressure provide for recoil forces, which can affect the melting bath strongly (melt ejection).
- *Dissociation and/or ionization:* As a result of the induced shock wave and the immensely high pressure and temperature rise above the surface, nitrogen molecules are dissociated as well as the ablated Ti- and gas-atoms are ionized. Besides, free electrons arise, which can cause the so-called "plasma shielding", which lead to the absorption of the laser beam in the plasma and a further heating of the plasma.
- *Gas adsorption and absorption:* Activated nitrogen above the surface is now available. This can be absorbed more effectively by the surface. This mostly takes place according Sievert's law (partial pressures), whereby approximations and deviations arise here.
- *Gas atomic transport (diffusion, convection):* If the nitrogen is within the metal (liquid/solid), then it is transported by diffusion or convection (ms time scale). After a sufficient time, a specific depth profile develops. Finally, depending on enthalpies the titanium nitride phase arise.
- *Nucleation and solidification:* After the nucleation processes certain solidification morphologies develop depending on gradients of temperature and concentrations at the solid–liquid interface. The grain size and

induced stress of these phases, now determines considerably the macroscopic characteristics, and at least the process result.

In order to be able to describe dependences quantitatively, first all measured variables must be called and defined. On the one hand one has to concern all parameters of the laser and its beam. The probably most important parameter here is the power density. The change of it is in most cases reached by variations of the spot size D_b. As next, one has to differ between pulsed- and continuous wave mode (cw-mode). They determine the energy incorporation, the temporal distribution and the interaction time. In relation to the cw-mode, the scan velocity v_s is the most important one, while in the pulsed mode the pulse frequency is determining the treatment. By the variation of geometrical scan parameter (lateral shift δ, spot size D_b, velocity v_s, pulse frequency f, number of scans n) it is arbitrarily possible to steer and thus to handle the total process. It allows that custom-made coating characteristics can be obtained by skillful combination of these parameters. A further parameter of the procedure is the gas pressure of the background gas nitrogen. It can amount to five bars, due to the experimental setup up, and affects finally crucially the process. The pressure dependence has been studied in recent publications [64–67] for other systems. To most neglected variable is the material itself. During the synthesis optical, thermodynamic and mechanical properties are modified and will be needed for the quantification of the process. Due to changes in the aggregate state, the characteristics are strongly modified. For example the description of convection of the liquid metal, parameters like the viscosity are needed. They all contribute the solidification behaviour and the quality of the functional coatings. Also the physical characteristics in the gaseous phase are important. Knowing them, the plasma composition and the nitrogen activation can be computed.

The classification of the time scales is very important, since the synthesis process must be assigned and its processes have to be related to correct "physics". For the investigations performed here, the range extends of femtoseconds, the duration of the shortest FEL- and Ti:Sapphire-laser pulses, up to minutes or hours in the case of macroscopic treatments. This nevertheless corresponds to approx. 18 orders of magnitude.

For the laser material processing on different time scales various investigations, overview articles [68] or books [5, 8] exist. In the case of fs-pulses the thermal description of the laser material interaction does not work. For this reason a two-temperature model was developed [69], which describes that process. In this review related effects like coulomb expansion and electron phonon coupling will not be discussed. The treatment with the ns-pulses of Nd:YAG- or Excimer lasers can be handled using the classical heating. This time scale refers already to very short interaction times and is an indication for small coating thicknesses. Times within the range of one microsecond arise for pulsed nitriding by means of FEL or nitriding in cw-mode (FEL, CO_2, Nd:YAG). In this case an efficient coating synthesis has to be expected. Convective effects can influence the process and determine the surface quality and the material transport. For example at cw-mode nitriding by means of FEL, the process duration at a surface element is about 10 ms. Strong surface deformations and problems with the homogeneity are expected. The processing time can be measured due to the used scan parameter. The expected duration differs from some seconds up to a few minutes per cm^2. This is shorter compared to the classical PVD procedures (hours).

3 Results

In this section experimental results and the modelling of several processes will be discussed. Most of the investigations are still published. In the first part the synthesis of TiN coatings using Nd:YAG laser gets instructed. The results were taken from own investigations [57, 58] and the literature [42–48, 51, 70–80]. The second part will discuss the process utilizing a free electron laser, a unique heat source with a special time structure. This part based on investigations published in [51–56, 59, 60]. At least a comparison of results using other commercial laser will be shown. This discussion contains results on CO_2 laser nitriding (taken from [24, 29, 34, 37, 41, 81–103]), Excimer laser nitriding [51, 67, 87, 103–109] and first investigations on a femtosecond Ti:Sapphire laser [51, 61]. At least the solidification behaviour gets classified into the valid theory. The basics of the experimental methods, the modelling data and the utilized models are explained in the respective publications and are not the object of the discussion.

3.1 Nd:YAG laser nitriding

The Nd:YAG laser used in [57, 58] operates in the first harmonic and is equipped with an optical scanner, which allows diverse relative movements of the beam. The scans were accomplished in a meandering fashion like described before. At least, the following parameters were used for the direct laser synthesis (Table 1):

The selected background nitrogen pressure P_A was selected during all experiments to 3 bar, since the most stable synthesis conditions were observed here. By means of the scanner the different geometric scan parameter were varied and optimized. A restriction was present however,

Table 1 Beam- and scan parameter during the Nd:YAG laser synthesis

Parameter	Symbol	Value
Wavelength	λ	532 nm
Intensity	$I_{0\text{-Nd:YAG}}$	8.8×10^{12} W/m^2
Average/pulse-power	$P_{Nd:YAGm/p}$	40 W/70 MW
Pulse energy	$E_{Nd:YAG}$	40 mJ
Frequency	$f_{Nd:YAG}$	100 Hz
Spot size	D_b	700–1.150 µm
FWHM (Gaussian)	$\tau_{Nd:YAG}$	6 ns
Scan velocity	v_S	1–5 cm/s
Lateral shift	δ	0.05–0.2 mm

the pulse frequency $f_{Nd:YAG}$ had to remain constant at 100 Hz.

3.1.1 Experimental results

3.1.1.1 Surfaces- and coating morphology-ns-pulses TiN has been successful synthesized shown in Fig. 3, where five example are represented. It is noticeable that they have a strong variation of the colouring and the optical characteristics. Based on it is already possible to provide information concerning the nitrogen content and the coating composition [110, 111]. The darker samples have a higher content of N-atoms. This is related to the changed number of free electrons in the matrix and the resulting dielectric function.

The SEM-micrograph in Fig. 3 gives a look at the structure. It is strongly determined by the overlap of the individual laser pulses. It has to be recognized a weak melt ejection at the edges of the interaction zones, what refers to the so-called Piston effect, which develops due to high recoil pressures. Similar observations have been done in [70, 72, 74]. The development of microcolumns was observed by György et al. [78, 79] at higher energies. Strong convective influences do not play a role for the surface quality, since the interaction time of some nanoseconds is too small. The different processes result in a roughness of approx. one micrometer (Santos et al. [72], −0.7 µm).

Figure 4 shows the different transverse cross sections of sample 2. The TiN - coating has a thickness of approx. two microns and is shaped by the heat flow and the melt movement due to the pressure. The more detailed TEM-micrograph (left) shows a granular composition of the coating with grain sizes within the range of 200 nm close to the surface. It is shown that this size drops down in deeper regions, which refers to reducing nitrogen contents within this range. The growth direction of the crystallites is perpendicular to the surface. Coating thicknesses of some microns (1–4 µm) have been measured in [51, 70, 72, 74] too. The short interaction time seems to limit the thickness.

3.1.1.2 Surfaces- and coating morphology-cw-mode/ms-pulses Such experiments have been performed in [43–48, 72] at cw-mode or in [42, 72, 73, 76, 80] at ms-pulsed mode. Man et al. [44, 46, 47] carries out experiments at cw—500 W and synthesized coatings of about 300 microns in thickness. They contain dendritic cubic TiN and show a very good erosion resistance. XPS-measurements verify the strong bonding at the nitrided region. Such dendrites have been observed by Golebiewski et al. [45] too. They measured residual stresses up to 800 MPa. A work of Labudovic et al. [43] tries to compute these stresses, induced during nitriding at cw—800 W. The simulations show comprehensive stress of about 600 MPa. Mori et al. [48] used a 50 W laser and a small spot size for the synthesis. His coatings have a thickness of about 500 nm. Further investigations have been carried out by Santos et al. [72]. They use a power of 50 W at a spot size of 0.1 mm and a scan velocity of 2 mm/s. Their coatings contain TiN and $TiN_{0.3}$ at a thickness of 60 microns. The surface quality is determined by cracks and a high roughness.

The experiments of Xue et al. [42, 76] have been carried out at 330 W and with 5 ms pulses having an energy of 1–3 J. After optimization of the scan parameter they got a coating thickness of 30 µm (crack free). The roughness has been measured to be about 2 microns. Further they show that preheating leads to a significant reduce of stress and cracks. The microstructure is dominated by needle like solidified TiN phases and dendrites. In [72] investigations on ms-pulses were realized too. They got coatings of 35 µm and a roughness of 0.94 µm. Cracks have been avoided by controlling the pulse energy and the cooling rate. Covelli et al. [80] used 2–10 ms pulses at energy up to 40 J. His coatings of nearly 100 µm contain dendritic TiN

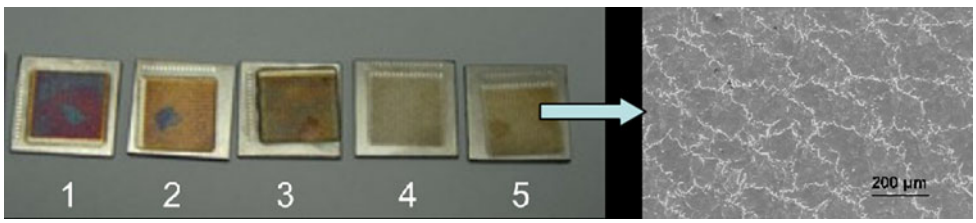

Fig. 3 Five typical synthesized TiN-coatings (from [57]), as well as a SEM-micrograph of a typical surface

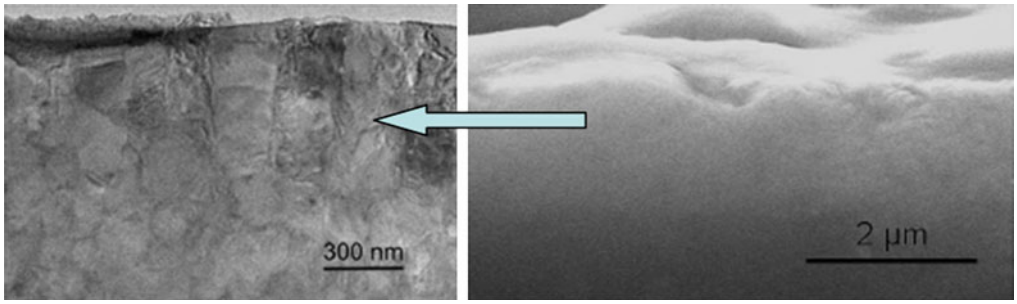

Fig. 4 Transverse cross sections of the sample 2 at TEM (*left*) and at SEM (*right*)

embedded in alpha-titanium. At deeper regions Ti_2N was observed. Very important is the alignment of the dendrites resulting from temperature gradients and the observation of convective effects on the transport mechanism and the coating properties. Ettaqui et al. [73] carried out experiments using 3 ms pulses at 50 Hz. His coatings contain undirected TiN dendrites up to a depth of 50 microns. All experiments show the possibility to tailor the process and will be used to draw the consequences.

3.1.1.3 Microhardness measurements Regarding the mechanical characteristics of the coatings and their technical and industrial applicability, microhardness measurements were accomplished by means of nanoindention. The measured hardness depth profiles of ns-pulse synthesized coatings in [57] are represented in Fig. 5. All depth profiles exhibit a steep rise of the hardness within the first hundred nanometres close to the surface. Then they reach their maximum value and drop finally slowly to the hardness value of the substrate.

The effect of the low hardness in the proximity of the surface results from the roughness of the samples, which likewise lies in the micrometer range and affects the measurements sufficiently [57]. Oxidation effects on the hardness profile at the surface could be neglected. They only have a small influence on the penetration depth [17]. The mathematical description and the analyses of the depth profiles using models gets explained in [57].

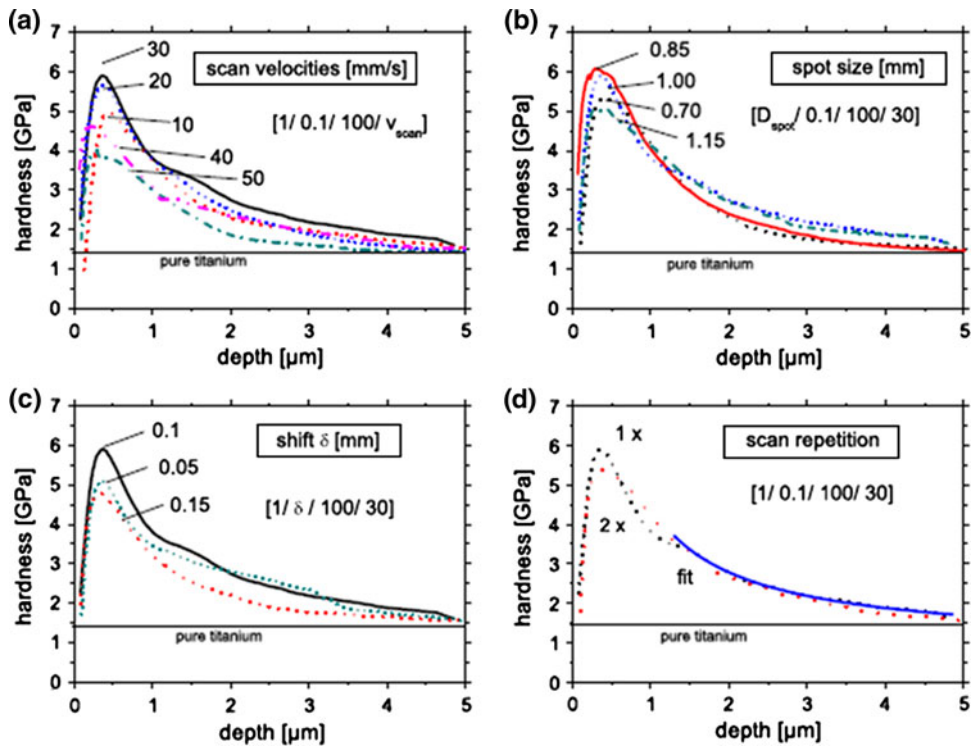

Fig. 5 Influence of **a** the scan velocity υ_{scan}, **b** the spot size D_{spot}, **c** the lateral shift δ, and **d** the scan repetition n on the measured hardness. In **d**, an example of a Jönsson and Hogmark [112] fit is shown (*fit*). For all plots, the parameters are given by the notation $[D_{spot}\,[\mathrm{mm}]/\delta\,[\mathrm{mm}]/f\,[\mathrm{Hz}]/\upsilon_{scan}\,[\mathrm{mm/s}]$ (from [57])

First the influence of the scan velocity is examined and it shows up that an optimum exists, which is with approx. 30 mm/s (Fig. 5a). These results from exceeding the melting threshold (similar to [74]), the increasing nitrogen entry and at least a balance between the energy entry and the acting forces. At high velocities the interaction time of the laser with a surface element is to short, in order to melt effectively and deeply, which leads finally to smaller coating thicknesses. Contrarily, remelting and convective effects occur at slow velocities, which induces stress and cracks and decrease the quality of the surface morphology. Changes of the spot size correspond to changes of the intensity/energy density. It can be assumed that with all used sizes the evaporation threshold was exceeded and therefore plasma was induced. This results from the very high pulse energy of the laser, which leads finally to the fact that only weak variations in the hardness measurements have been observed. The influence of the lateral shift is similar to that of the scan velocity. The maximum hardness was observed for a lateral shift of 0.1 mm. Again the principle of the balanced conditions and a moderate energy entry is valid here. Figure 5d shows the measured hardness profiles of two samples treated with the same parameters, but the number of scans n was changed. For n = 2, a repetition of the treatment, no significant changes have been observed. That shows that it is unnecessary to accomplish several scans on a sample since the absorption of nitrogen is already satisfied. Only a change of the nitrogen profile in deeper regions is observed. Using the model of Jönsson and Hogmark [112] the pure coating hardness is bigger than the measured maximum hardness. It reaches values of up to 12 GPa, which in technical regard is outstanding, however still smaller than with alternative procedures such as PVD.

Xue et al. [42, 76] measured a hardness of 13 GPa for coatings synthesized at ms-pulse mode. The results of Ettaqi et al. [73] show a hardness of about 1700HV0.2 (∼) which is close to the results of Santos et al. [72] who measured a value of 1600HV0.2 (∼). Mori et al. [48] determined a hardness of 14 GPa at his cw-mode coatings. The analysis of coatings from Man et al. [47] shows values of 2000HV0.2 (∼) on his samples. All measurements present a strong increase in hardness, but not the value of pure TiN of ∼25 GPa. The inhomogeneity of the coatings and the embedded dendrites at thicknesses about ∼50 microns are the remaining problems.

3.1.1.4 Nitrogen depth profiling The RNRA-measurements [57] in Fig. 6 show diffusion-like depth profiles, which are limited to approx. 500 nm due to the limited information depth. Thus one does not receive the complete nitrogen distribution in the TiN-coatings. However, it is noticeable immediately that approx. 50 atm.% nitrogen close to the surface is available. Stoichiometric TiN phase formations now can proceed. A similar result was observed in a study of György et al. [75].

The mathematical description of the diffusion has been evaluated in [57] in detail. Because of the temperature dependence of the diffusion coefficient D(T), an average coefficient of $2 \times 10^{-4}\mathrm{cm}^2/\mathrm{s}$ has been used. It refers to investigations in [59] and of Shuja et al. [113] performed at temperatures of the melt close to the boiling point. Investigations of Labudovic et al. [42] for the gas nitriding of Ti6Al4V show a similar value of 4.4×10^{-4} cm^2/s.

Depth profiling has been also performed by other researchers. Most of them used XPS in combination with sputtering to get information about the chemical composition of the coatings. Man et al. [44, 46] observed a nitrogen content of approx. 40 atm.% in his system. Similar observations have been carried out by Santos et al. [72]. All researchers found non-stoichiometric TiN_x (1>x>0.6) embedded in alpha titanium containing nitrogen in solution.

3.1.1.5 X-ray diffraction Diffraction experiments are widely used to get detailed information about the

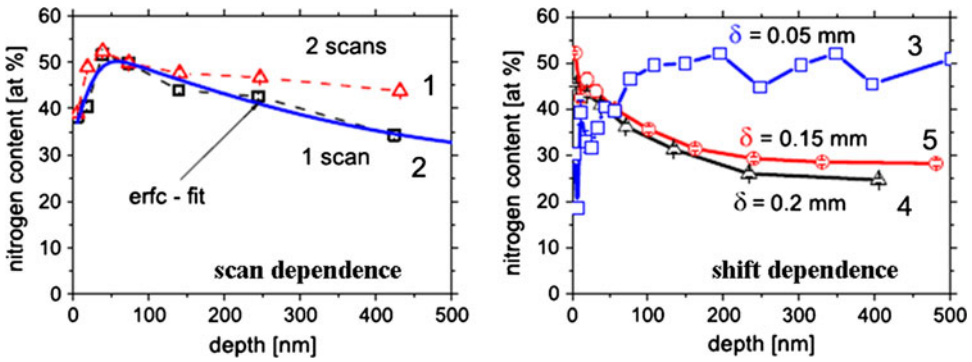

Fig. 6 Nitrogen depth profiles for two scans n (*left*) as well as for different lateral shifts (*right*) with the following parameters ($n, D_b = 1\,\mathrm{mm}, \delta = 0.05 - 0.2\,\mathrm{mm}, \upsilon = 30\,\mathrm{mm/s}$ and $f = 100\,\mathrm{Hz}$), from [57]

microstructure of crystalline systems. In this case extensive analyzes have been performed to get information about stress, strain, grain sizes, lattice parameters or textures. Own investigations on ns-pulse nitrided titanium have been published in [58]. The investigations show the development of the lattice strain, the grain size and the texture depending on the scan parameter. The strain was minimized to a value of 0.002 at grain sizes up to 200 nm. It was shown that the development of a (200) texture correlates with the induced strain. Wu et al. [70] used XRD to determine the composition of the nitrided zone and to measure the lattice parameter a of the TiN. a was measured to be 4.24 Å which is close to the literature value of 4.241 Å of stoichiometric TiN [114, 115]. Santos et al. [72] measured this parameter too and used grazing incidence scans to determine the coating thickness. Their measurements show smaller values. This is a hint for non-stoichiometric phases. The analyses of György [74] uses XRD to verify the Ti_2N phase in the coatings.

Man et al. [47] used grazing incidence scans to determine the composition of his, in cw-mode synthesized, coatings. They only show cubic TiN. Mori et al. [48] measured a lattice parameter of 4.231 Å in his coatings having a weak (111) texture. Their diffraction pattern also shows just TiN and alpha titanium. Experiments on ms-pulse mode produced TiN have been carried out by Ettaqui and Xue et al. [42, 73, 76]. Ettaqui shows the development of cubic TiN and a small content of hexagonal alpha-titanium nitride ($TIN_{0.3}$). The investigations of Xue presented similar results. Additionally, the alignment of TiN in (200) direction was observed. Summarizing, the possibilities of XRD offer lots off data and results which should not represented here and are available in the literature. It is important that all results correspond each other.

3.1.2 Modelling the process

The process should be regarded here from the theoretical side for nanosecond treatments to determine process variables, which are experimentally with difficulty access, by means of simulations. The most important ones are the surface temperature, as well as the melting- and diffusion depth. Interesting should be also, how the vapour pressure affects itself due to the ablation at the surface.

3.1.2.1 Melt- and evaporation behavior For the better process understanding regarding melting depths and phase formation, it is important to know the temperature distribution in the substrate during the irradiation. From this, conclusions can be drawed on the coating characteristics and it offers the possebility to do comparisons with the experiment. The modelling took place by means of the heat equation, however under neglecting convective effects and external losses of energy, but with inclusion of the evaporation processes via a loss term on the edge [116].

The Nd:YAG laser is as a Gaussian like heat source (temporal, spatial) with corresponding spot size (D_b) and an intensity $I_{Nd:YAG}$. In the computations are besides contained the phase transitions of the titanium. All material properties were already introduced in the literature [54, 56, 57]. The reflectivity of the titanium with the used wavelength amounts to approx. 50%. In Fig. 7 the different results of the computations are represented. During the first nanoseconds a very fast overheating of the titanium was observed. Ablation conditions are reached and the surface temperature rise immediately about 5,000 K. This leads to a strong plasma and finally to the increase of efficiency of the synthesis by the nitrogen activation. The melting duration of the titanium amounts to about 40 ns. During this time most nitrogen is absorbed and transported into the titanium. The melting depth for such 6 ns pulses lies with approx. 500 nm and is somewhat smaller than the coating thicknesses measured in the experiments. Since by the overlapping treatments several times melting occurs. It can be proceeded from an effective melting depth of a micron. For TiN this value fails smaller. It amounts to something like 100 nm.

Figure 8 represents, that the titanium is loaded strongly by a recoil pressure ($P_{recoil} = 0.55\ P_S$). Due to the high temperatures a high saturation pressure is induced above 100 bar on top on the surface. The resulting recoil is enormous and induces a shock wave in the substrate. Besides melted titanium becomes affected by the so-called

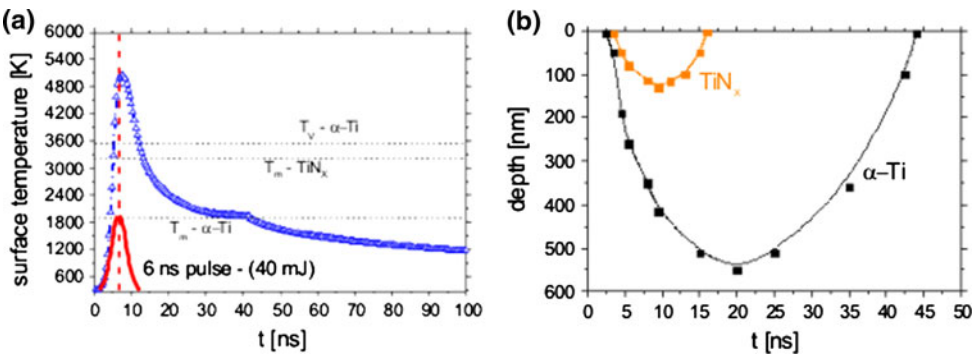

Fig. 7 Surface temperature **a** and melting depth **b** during irradiation of titanium with 6 ns Nd:YAG Laser

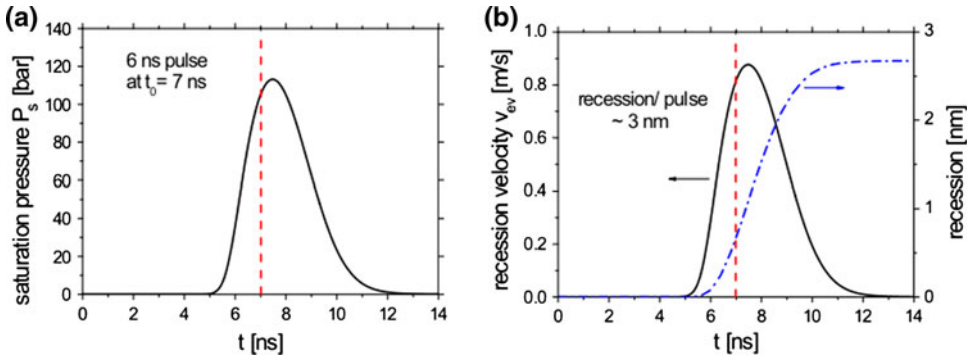

Fig. 8 Saturation pressure **a** and material removal and its speed of **b** during the irradiation of a 6 ns laser pulse

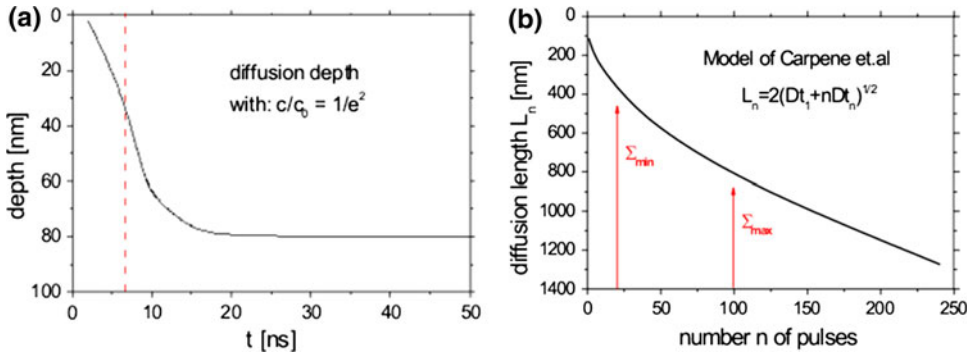

Fig. 9 Diffusion depth (drop of the concentration to $1/e^2$) for the irradiation with Nd:YAG laser pulse **a** as well as the diffusion length L for the irradiation with n pulses **b** according to the model of [49]. D and t correspond to the respective diffusion coefficient and times. Σ corresponds the overlapping in the experiments

"Piston-effect". This squeezing out leads to the reduction of the surface quality. The computations show further (Fig. 8b) that the material removal takes place with a speed of approx. 1 m/s. Per pulse about three nanometers are removed, which sounds negligibly. However, if one regards the synthesis procedure and proceeds from the overlapping tracks, then this can add up fast to some hundred nanometers.

3.1.2.2 Nitrogen transport It is clear that due to the order of magnitude of the time, a purely diffusion-dominated coating development was observed. For this reason the diffusion depths were computed by means of second Fick' law. They permit a view of the transport mechanism to the N-atoms and show, how the coatings develop. The following Fig. 9 shows the computed diffusion depths.

As diffusion coefficient D (T) the relation of Wood et al. [117] was used. The diffusion depths is defined as the concentration, where c drops down to an amount of $1/e^2$ from the opposite maximum. For one pulse (Fig. 9a) the diffusion length has been calculated to reached approx. 100 nm. That is much smaller than the observed coating thicknesses. Since by overlapping the laser spots each surface element was treated several times. The real diffusion depths are much larger. In order to describe this quantitatively, it is necessary to use a model, which describes this adequately. The work of Carpene et al. [50] introduced a model, which computes the diffusion length L for multi-pulse irradiation of iron:

$$L_n = \sqrt{4(Dt_1 + Dt_n)} \quad (1)$$

D corresponds to the diffusion coefficient, n the pulse number and t the diffusion times. D was accepted simplifying for computation constantly to 2×10^{-4} cm^2/s, according to the RNRA-investigations. The value Dt_1, which describes the diffusion behaviour during the first pulse, can be taken over from simulations and their result (Fig. 9a) (approx. 1.6×10^{-15}). t_n corresponds the diffusion time during the multi-pulse irradiation. It corresponds to the melt duration of the titanium of 35 ns (taken from simulations). Figure 9b shows very well, the irradiation with several pulses and its influence on the coating thicknesses. The computed depths correspond approximately to the measured thicknesses.

3.2 Free electron laser nitriding

First experiments using such a laser has been carried out and investigated in [51–56, 59, 60]. The functionality of the used FEL at Jefferson lab is described in [118, 119]. It works with femtosecond pulses at high frequencies. Continuous fs-pulse trains are also called cw mode. The pulses can also be compressed into pulses of some milliseconds known as pulsed mode. The following Table 2 summarizes the used laser- and treatment parameters.

Table 2 Scan- and process parameters used during the treatments at the different modes

Parameter	CW	Pulsed
Wavelength range (microns)	1.6	3.1
Bunch length (FWHM psec)	0.2	0.5
Laser power/pulse (micro Joules)	125	20
Laser power (W)	650	160–750
Repetition rate (cw operation, MHz)	4.68	37.4
Scan velocity v_{scan} (mm/s)	24	0.5
Spot size D_b (microns)	600	440
Lateral shift δ (microns)	400–2,000	100–200
Macro pulse duration (μs)	–	250–1,000
Gas pressure (atm.)	1.15	1

3.2.1 *cw-mode experimental results*

Such experiments have been described in [54, 60]. As demonstrated in Fig. 10 a melting track occurs during the irradiation. The nitrogen reacts with the melt and the synthesis of titanium nitride takes place. They got a golden like color and are quite inhomogeneous.

As expected, the track properties are mainly determined by the melt flow. Marangoni convection and pressure induced melt modifications resulted in a strong roughness. Humps and melt ejection were not being observed. Further a periodical structure is visible as a result of the equilibrium of the surface acting forces. Short wavelength structures could be observed too. Due to the oscillations on the liquid titanium such modifications are developed. They are formally known as Rayleigh–Taylor instabilities.

Numerical studies have shown a strong influence of the convection on the track or respectively coating properties [54]. The Marangoni force induced flow velocities up to 1 m/s. Convective heat transfer becomes the main determining process. The describing number in fluid mechanics is the Peclet number (Pe). It reaches values about 60. That is the reason for the low aspect ratio of the melted tracks. Further the diffusive nitrogen transport can be assisted by the convection. Due to the mixing in the liquid pool the coating thickness will be determined by the melting depth. In the shown examples this depth was about 200 microns.

Nitrogen depth profiling using RNRA (Fig. 11) verifies stoichiometric TiN using overlapping tracks. XRD measurements in Bragg–Brentano geometry show that only δ-TiN has been developed. Depending on the lateral shift the texture development was observed. Figure 11 presents the diffraction pattern of the selected samples with multiple tracks at a spot size of 600 microns. The virgin α-Ti was observed too, but at a low content.

The Bragg–Brentano scans on the right-hand side at Fig. 11 show a strong [200] peak which indicates the development of a weak [200] fiber texture. As a result the titanium nitride lattice is directed perpendicular to the surface.

Cross section micrographs have been performed too (Fig. 12) in order to take account the phase formation during solidification. They show the redirected TiN dendrites near the surface. Their distribution is quit inhomogeneous due to the varying temperature conditions during the treatments. The hardness measurements on the right-hand side verify the dependence of hardness on the nitrogen content and at least on the phases.

3.2.2 *Pulsed-mode experimental results*

These experiments are described in [51–53, 55, 56, 59]. During the treatments coatings with very varying properties and thicknesses up to 20 microns have been generated. They got interesting and correlating properties to their scan and beam parameters. The most presentable sheets have been investigated and are studied as next. Their scan parameters are shown in Table 3.

Most experimental results are available in [52, 53, 55, 59]. Carpene et al. [51] shows first tries to synthesize TiN directly using FEL radiation. [56] is a theoretical publication

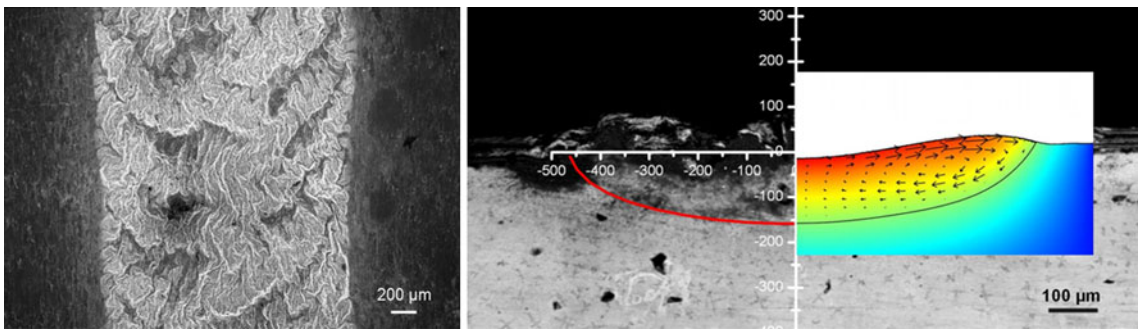

Fig. 10 Nitrided tracks in top view and as cross section (taken from [54]). The simulations describe the surface deformation due to the Marangoni convection and the melt pool shape

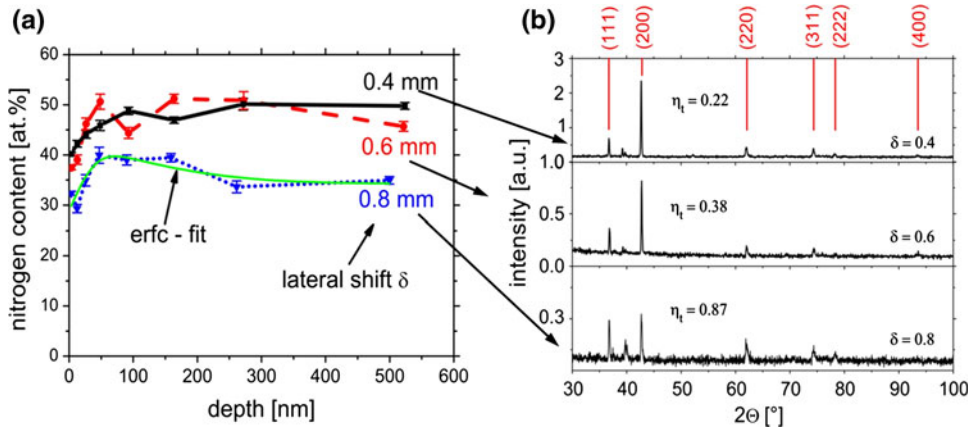

Fig. 11 Nitrogen depth profiles using different lateral shifts δ (*left*) and their corresponding diffraction pattern (*right*) (from [60]). η_t describes the intensity ration of the (111) to the (200) peak and is known as the texture parameter

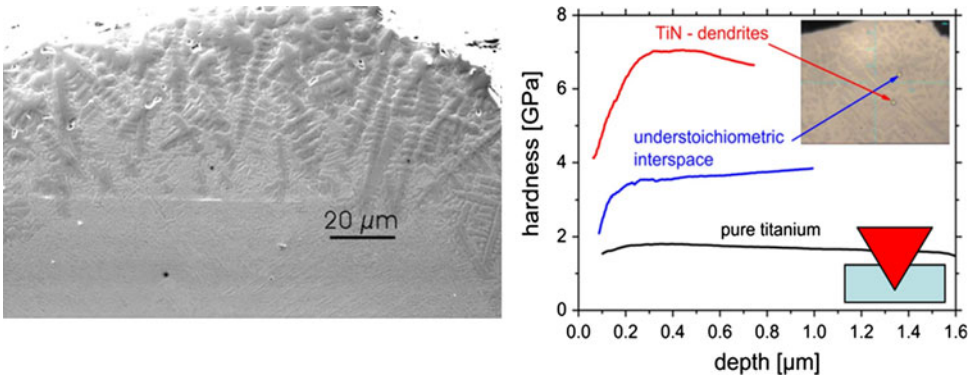

Fig. 12 Cross section micrographs of titanium nitride and hardness measurements at different regions (from [60])

Table 3 Macropulse duration τ_{ma}, macropulse repetition rate f_{ma} and lateral shift δ (in y-direction) used for the FEL treatments. The scan velocity in x-direction is 0.5 mm/s

Sample	τ_{ma} [µs]	f_{ma} [Hz]	δ [µm]
1	250	60	100
2	750	30	100
3	1,000	30	100
4	1,000	10	200

containing information about plasma development during the irradiation.

The surface properties are very different and show a strong dependence on the scan parameters. Figure 13 presents SEM micrographs of the coatings. Sample 1 and 2 got solidified melting droplets and some cracks as a result of the remelted titanium and the resulting induced intrinsic stress. For longer macropulse durations melting droplets could be avoided as a result of exceeding the evaporation point. The energy entry for sample 3 was four times higher then for sample 4. As a consequence sample 3 got many cracks and was still fragile. In technical point of view sample 4 has the best properties. The coating is relatively smooth and without any fractures.

In order to understand the melting behavior, numerical simulations have been performed by means of the finite element method (FEM). Heat transfer and phase transitions were studied. Detailed information is available in [55, 59]. The results show that the surface temperature during the treatment determines the properties.

Figure 14 shows the temperature distribution during one macropulse. For longer pulse durations the surface temperature is high enough to evaporate titanium and to remove the droplets. The increase in coating quality is a main result of the observations. Profilometrie of the samples shows a decreasing roughness R_a from 3 to 1.2 microns.

In relation to mechanical loading the coating hardness is the most important parameter. Wear resistance and friction coefficient can be improved in order to optimize several components or assemblies in technical applications. Figure 9 presents the results obtained for the selected samples. Due to the bad surface quality (rifts, droplets) samples 1–3 are very inhomogeneous. Sample 4 shows a strong improvement of the overall hardness to 8 GPa (film hardness 12 GPa). Those properties are mainly determined by the phase transitions which are strong related to the nitrogen content. For maximal optimized coatings, stoichiometric TiN (50 atm.%) has to be synthesized. Therefore, the RNRA measurements show results in agreement to that. At Fig. 15 the stable titanium nitride was observed over the whole measured range.

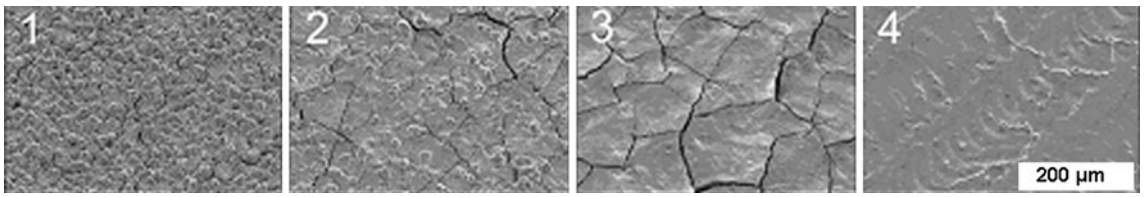

Fig. 13 Surface properties of selected samples. (from [55])

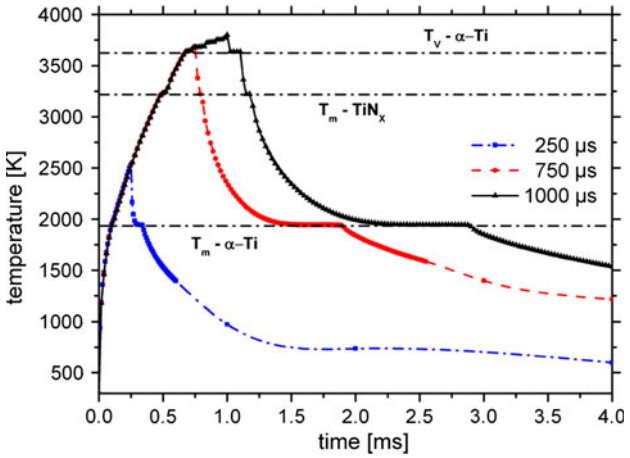

Fig. 14 Surface temperature development during a macropulse [59]

Additional EDX investigations show the diffusion like profiles at deeper regions.

X-ray diffraction measurements resulted in correlating lattice properties. The development of a strong 200 fiber texture was observed by means of Bragg–Brentano and Rocking curve scans. Figure 10 shows that orientation behavior assisted by pole figures (Fig. 16).

Those diffraction patterns verify the development of a fiber texture in (200) direction. The directed lattice seems to be the reason for the improved mechanical properties and its strength. Cross sections and solidification behavior will be discussed in Sect. 3.4. The synthesized coatings show the possibilities of such treatments.

3.3 CO_2-, Excimer- and Ti:Sapphire laser nitriding

3.3.1 CO_2 laser nitriding

CO_2 laser have been selected at the first time to produce TiN in a reactive ambient. Since then the method was applied in most cases using this kind of laser. All experiments using lasers up to 3 kW showed the development of coatings of about 500 microns in thickness [23, 25–28] and a hardness of 2000HV0.2. All observed dendritic solidification close to surface. Ursu et al. [24] and Katayama et al. [22] performed first experiments using pulsed treatments. Ursu et al. synthesized coatings of 40 microns under 2 bar nitrogen. The millisecond irradiation of Katayama led to a hardness of 700HV0.1. Morton et al. [31, 32], Ignatiev et al. [30] and Mridha et al. [33] performed further experiments. They got coatings of 200 microns. Last one observed the influence of capillary forces on the process. Their coatings got hardness of 2000HV0.2 but at a worse surface quality. Hu et al. [29] and Xin et al. [34, 85] used a spinning laser beam in order to improve the treatment efficiency. They also observed dendritic solidification. Xin showed the development of a (200) texture during his treatments. The surface had a roughness of approx. 2.7 microns but also cracks. Bonss et al. [36, 96] carried out extensive analyses on the nitrided titanium. It was shown that friction, sliding and all other important properties get improved. Nitriding experiments of Kloosterman et al. [37, 38] resulted in needle like dendritic solidified tracks of 100 micron in thickness. An alignment in top down

Fig. 15 Hardness depth profiles [59] as measured by nanoindention technique and nitrogen depth profiles

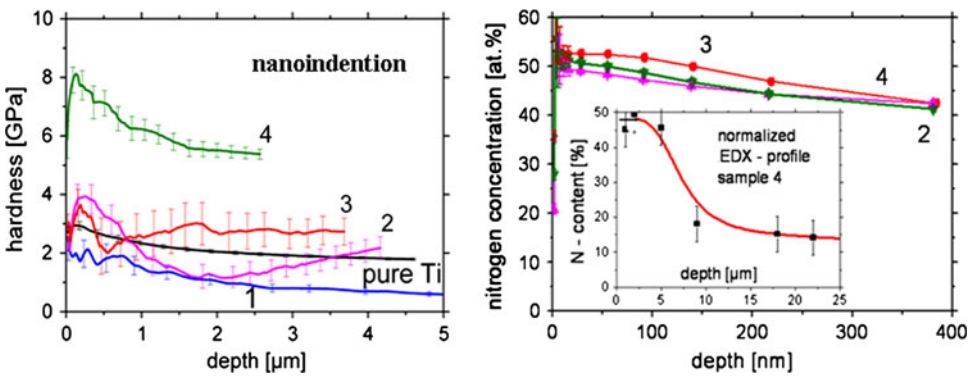

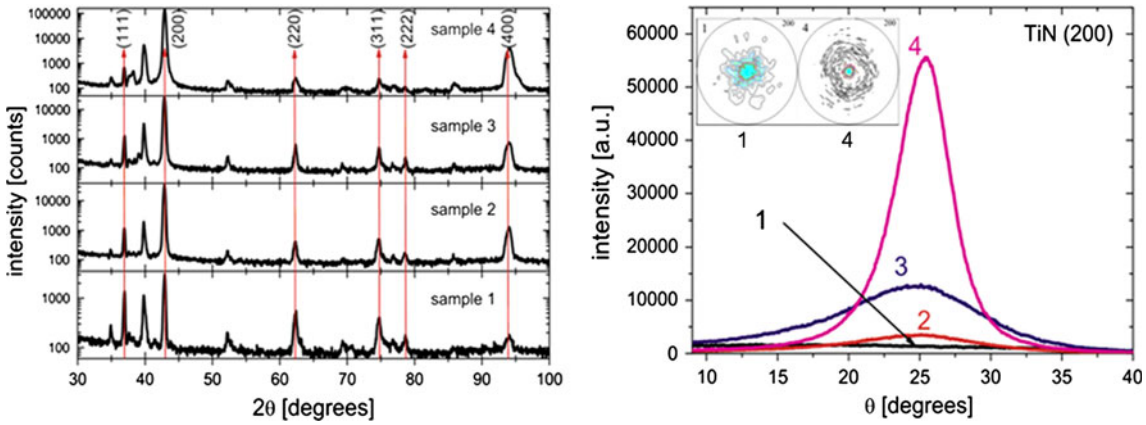

Fig. 16 Θ–2Θ scan, rocking curve and pole figures of the four selected samples. All indicated peaks are cubic TiN, the others belong pure titanium from [59]

direction was observed. Their hardness measurements showed similar results then earlier investigations of 1800HV0.2. Extensive studies of coating formation were done by Raaif et al. [101]. Figure 17 shows a typical cross section of his coatings of about 500 microns in thickness. The coatings have a hardness of about 10 GPa and a roughness of 7 microns. XRD investigations verify a (200) texture.

A very interesting and extensive work has been published by Nwobu et al. [41]. They did many parametric studies using a 2KW laser. The surface hardness was measured to be 1900HV0.2. They also performed simulations of the melting- and transport processes. Convective effects have been verified. In [84, 99, 100] Hu and Baker used overlapping laser tracks to treat areas. They studied the influence of preheating on crack formation and on the hardness during nitriding with 2KW laser power. The hardness was increased up to 800HV0.1. Numerical studies show the correlation between melting depth, coating thickness and hardness depth profile. Nice investigations have been done by Abboud et al. [83] where he produced crack free coatings with 800HV0.1. Parameter studies showed the possibilities of tailoring the method. Garcia et al. [82] did high power treatments of Ti6Al4V and synthesized dendritic coatings of 500 micron in thickness. Baker et al. [86] performed treatments under different nitrogen/argon gas mixtures. The coatings of about 500 microns got 700HV0.1 and a roughness of 3 μm after irradiation in 20% N-content. Very special investigations were done from Laurens et al. [94, 102] who studied solid state nitriding. The laser has been used as a preheating source. It was shown that the kinetics obey a parabolic growth law. Without melting thicknesses up to 5 microns developed after 15 min. (1,000°C). The studies give a detailed insight into the reaction kinetics. Thomann et al. [87, 103] did experiments using 300 ns pulses at 10 Hz and fluences up to 25 J/cm^2. He shows the creation of stoichiometric TiN of some microns in thickness. Actual experiments have been done by Yu et al. [81] who used moderate energy density to synthesize coatings of approx. 80 microns. His extensive diffraction experiments showed the presence of different stable titanium nitride phases (TiN_x, Ti_2N etc.). These phases have been measured by Yilbas et al. [88] too. His coatings are crack free and needle like solidified. Xin et al. [89] again carried out experiments at 2.8 kW and under 80/20% nitrogen/argon mixture. Fast scans (10 mm/s) at high energy densities led to $TiN_{0.8}$ in a range of 50 microns. The resulting high cooling rates led to finer structures of the dendrites. Other investigations have been done by Mridha et al. [33, 90] at 1.4 kW. The influence of the scan velocity has been studied. A maximal hardness of 2200HV0.2 was reached with thicknesses of about 250 microns. Crack free and smooth surfaces have been produced at the highest scan

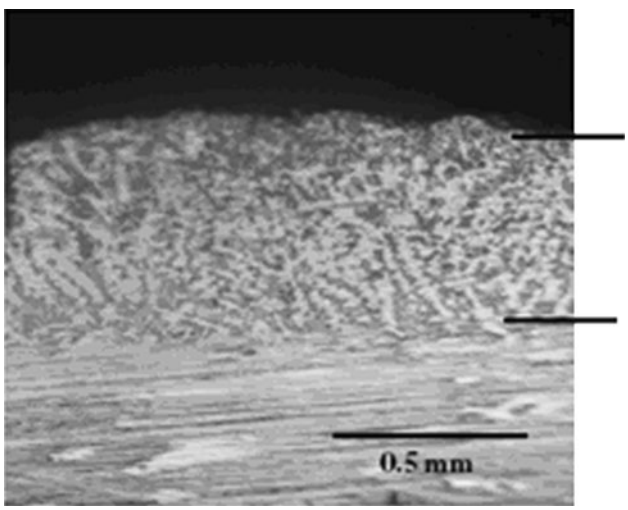

Fig. 17 Cross section micrograph of CO_2 laser nitrided titanium (from [101])

velocity. The microstructure was also needle like and dendritic. Kaspar et al. [92, 93] carried out the synthesis method with Ti6Al4V. Experiments with 3.1 kW showed the development of TiN_x up to 300 microns and a hardness of 900HV0.1. They optimized the development of cracks. It was shown that to large dendritic structures decrease the mechanical properties in relation to technical applications. Jianglong et al. [95] did experiments at a high background pressure of 4 bar and with 1 kW laser radiation. They got 400 micron thick dendritic coatings having a roughness of about 2 µm. Other investigations of Bonss et al. [96] at very high energies (6 kW power) showed thickness up to 1 mm and a hardness of 1200HV0.1. The tribological properties of their coatings are excellent. An other investigation of Weerasinghe et al. [97] with 2 kW showed the development of 600 micron thick coatings. Due to preheating the hardness was measured to be 950HV0.1. Remelting effects have been studied and explained. It led to better coating properties and an improved corrosion resistance. The synthesis of TiN by Zimnicki et al. [98] results in coatings of about 200 microns and a hardness of 2600HV0.05. Typical dendritic solidification was observed containing TiN and Ti_2N. Calculations of the melting depth verify the dependence of the coating thickness on it.

Comparing all results the process seems to be limited. The coating thickness never exceeds one millimeter. The hardness strongly depends on the phase formation and was always below the hardness of perfect TiN. Dendritic solidification determines the microstructure as a result of the cooling rates. From technical point of view surface quality, cracks and inhomogeneity remain the main problems. Later comparisons will show the independence of such behaviours on the type of laser.

3.3.2 *Excimer laser nitriding*

Soft UV radiation has been utilized from D'Anna et al. [104, 105], Thomann et al. [87, 103], Mihailescu et al. [107–109] and Carpene and Han et al. [51, 67] to synthesize TiN in nitrogen atmosphere. D'Anna used a XeCl laser (30 ns) at 0.6–1 J/cm^2, 50 Hz and 1.1 bar to perform his experiments. He shows the formation of titanium nitride of deposited titanium on silicon. Synthesis on pure titanium substrates show bronze-yellow coloured surfaces with a roughness determined by the multipulse scans. The coating thickness is about 200 nm having a hardness of about 6 GPa. NRA and RBS measurements showed the increase of the nitrogen content in deeper region correlates with the number of pulses. It was hinted the whole process gets determined by the liquid phase.

The experiments of Thomann et al. were carried out with the same kind of laser like before at 1 bar. The Fluence was varied between 1–4 J/cm^2. After multipulse irradiation coatings up to 2 microns have been created having a roughness of 0.5 micron. XRD showed the creation of δ-TiN. Additionally, the plasma composition was measured. They verify the strong dependence of phase formation on the induced plasma. In the work of Mihailescu et al. a XeCl laser was used at a fluence of 5 J/cm^2. In [109] they studied the dependence of the background pressure on the process. It was shown that the hardness could exceed values up to 11 GPa. Similar investigations of them showed the same results. They verify the need for induced plasma.

Carpene et al. [51] investigated the TiN phase formation in relation to other lasers. Han et al. [67] showed the synthesis of about 400 nm thick coatings at 2 bar and at a fluence of 4 J/cm^2. All experiments show a high nitriding efficiency using such lasers. This seems to be related to the high energy coupling in the UV range, especially of titanium. Figure 17 verifies the rise of nitrogen content due to repeating irradiations.

3.3.3 *Ti;Sapphire laser nitriding*

Such experiments can be called "femtosecond nitriding". Those investigations were done from Carpene et al. in [51, 61]. The results show an inefficiency of the process. Due to the short interaction time and direct ablation the nitriding effect becomes disturbed. The duration of efficient melting, absorption and diffusion is to short. Only the surface gets treated and modified in a roughening way. Figure 18 describes that effect at hardness measurements. The properties of the samples were strong decreased. (Fig. 19).

3.4 Something about solidification

If one regards the entire synthesis process, then it becomes clear that one of the most important procedures is the

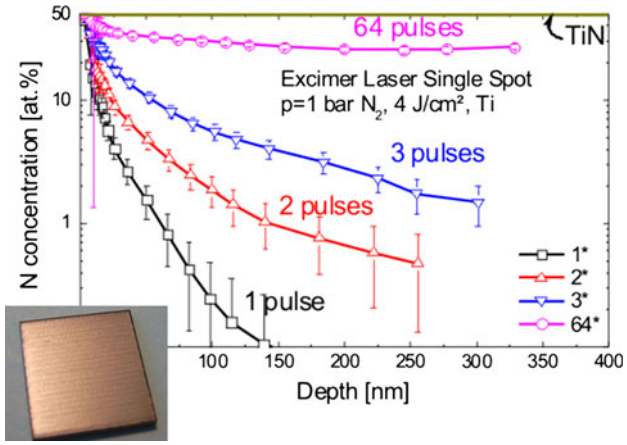

Fig. 18 Laser nitriding at different pulse numbers with a XeCl laser (308 nm, 55 ns, max.20 Hz area velocity: v area $\sim$2 cm^2/min)

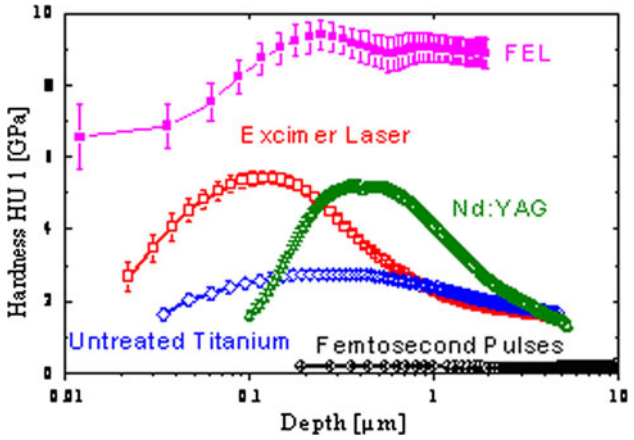

Fig. 19 Hardness of Ti:Sapphire laser nitrided titanium in comparison to other laser treatments

solidification. Finally, it determines the coating characteristics and the morphology. In the Bible of solidification physics [120] the basics of the phenomena taking place are represented. Some experiments and investigations are concerned also on the solidification behaviour in melting baths [121, 122]. All show the fact that the high cooling rates determine the characteristics of the coatings, that is the phase formation, their distribution and size as well as their morphology. In principle the solidification process can be described by three parameters:

1. Cooling rate $\varepsilon_c = \frac{dT}{dt}$
2. Velocity of the solidification front υ_s in normal direction of the solid–liquid interface
3. Temperature gradients G in normal direction $\left(G = \vec{n}\nabla T\right)$

These parameters can be taken from the computations or simulations. Here, the investigations are applied on the FEL treatments. Simulations resulted in a velocity of the solidification front of approximately 3 cm/s within the pulsed treatments and of 6 cm/s during cw-nitriding. The temperature gradients G were determined to be approximately 10^7 K/m in both systems. It is clear that the values vary strongly and are dependent on the position in the melting pool. The cooling rates are to be numbered with approximately 2×10^5 K/s. The following equation is valid now: $\varepsilon_c = Gv_S$. It is shown in [8, 123] that if ε_c becomes smaller, more roughly structures of the rigid phase have to be expected. However, the solidification morphology depends on the ratio $R = G/v_S$.

By means of these data the FEL nitriding can be applied very well into the generally valid theory of growth processes, which is impressively confirmed in Fig. 20 [right]. As one sees, the experiments agree very well with the theory. The expected aligned dendritic solidification in very fine structures was observed. The dendrites are equiaxed and got side branching respectively arm spacing in deeper regions. Surprisingly, it is aligned from the surface in top down direction, which is not observed in most other metallurgical investigations, since this always happens toward the liquid phase.

An explanation supplies Fig. 20 [left]. Due to the large differences of the thermal characteristics of pure titanium and TiN (difference in melting temperature of Ti and TiN of about 1,250°K) the solidification starts at surface, as the isotherm of the fusion point of TiN verifies. From the rigid structures it is possible to receive more exact information about the process. By means of the primary and secondary arm spacing of the dendrites the possibility exists to receive thermodynamic details of the structure formation [124]. Due to the complexity of the process and also its modelling (phase field model) a detailed study for the TiN system would be desirable in the future.

Dendritic solidification seems to be the main mechanism during irradiation of titanium using a free electron laser. Furthermore, the results can applied on nitriding utilizing other types of laser. As one sees at the CO_2 experiments

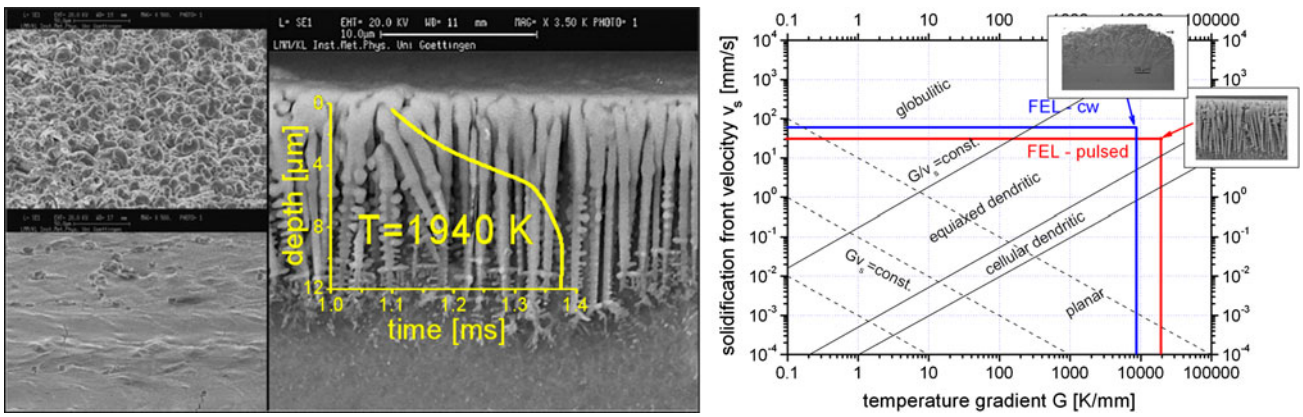

Fig. 20 Solidification behaviour, melting temperature isotherm (TiN) of pulsed FEL nitrided titanium [*left*] and classification of the solidification behaviour [*right*] of FEL laser nitrated titanium into the theory in [120]

(for example from Kloostermann et al. [37, 38] where aligned dendrites were observed) or for Nd:YAG laser synthesis like from [80], the solidification depends on the explained parameters and at least on the interaction time (in all cases some milliseconds). Due the knowledge of G and R it is possible to control the solid structure and at least the tribological properties.

4 Conclusions for the whole process

4.1 Parameterizing the method

Overlapping laser tracks were already used for nitriding of areas like in [29, 84, 99, 100], but are still not quantified. As the experiments in [57, 59] showed, it is possible to summarize the different geometrical scan parameter. As a result the overlap-parameter Σ was defined, since it summarizes and simplifies the different parameters of nitriding:

$$\sum = n\frac{D_b^2 \cdot f_{pulse}}{v_s \cdot \delta} \tag{2}$$

This parameter is dimensionless and describes how often each two dimensional surface element gets irradiated by the laser beam. A disadvantage of Σ is that it is purely geometrical, thus no information about temporal dependences or about the energy coupling are considered. However, if during an experiment the same laser beam parameters are used, very good correlations can be determined. Due to multiplying Σ by the respective pulse energies, then one receives a parameter, which describes, how much energy per two dimensional surface elements was incorporated. An example for parameterizing will be shown as next in the case of Nd:YAG experiments. Only the overlap Σ is necessary, because time- and pulse characteristics are to be regarded as constant.

Figure 21 shows the functional dependence of coating hardness and thickness on the overlap parameter. Some fluctuations were observed. They based on the multiplicity of interaction effects, which taking place during the treatment and are usually non linear coupled. At the experiments a rise of the internal stress gets observed, due to the rising energy entry and the following thermal loads in the material. The fact that the coating thicknesses increase during more intensive surface treatments, results from the rising melting depths as well as more efficient nitrogen transport. For the hardness measurements exists an optimum of Σ for the treatments. In this case balanced conditions between acting processes like melting, cracking etc. were reached.

It is possible to use these parameters for several different kinds of treatments. The example should only give an insight into the possibilities to tailor the method. Since then it should be more attractive from industrial point of view. Further developments should start at this purchase.

4.2 Competitive process variables

If one regards the entire experiments, simulations and analyzes, then it is noticeable that the synthesis result, that is the TiN-coatings, never have reached an optimum of its characteristics at a firm set of parameters. It always exist a range of treatment parameters, in which acceptable results are obtained. However, if one deviates from that range, then the coating quality decreases seriously. These deviations are always based on to high or to low energy entry. Referring this information to the used lasers it is possible to set up "a for and an again" for the use of the respective experiment. It is like always in physics: an improvement of a characteristic always happens at the expense of another. The simplest example here is probably the coating thickness. In order to increase that one, more energy has to be incorporated, in order to increase the melting depth, nitrogen transport and so on. However, at the same time this leads to higher internal stress and to a worse surface topology due to the well-known effects. Such a physical process is convection. On the one side it supports nitrogen transport into deeper regions of the material, on the other side it leads to melt flow and to deformations of the surface. It can come even so far the fact that turbulent and

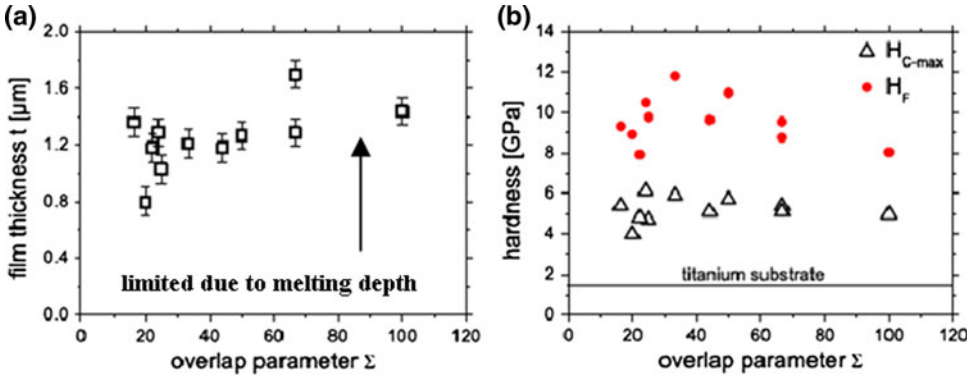

Fig. 21 Dependence of the film thickness (**a**) and the film hardness (**b**) on the overlap parameter. The thickness seems to be limited by the melting depth ($\sim 2\ \mu m$). The maximum hardness was measured close to $\Sigma = 30$, where the balance between induced cracks and melting is optimal (from [57])

chaotic processes arise and thus the coating characteristics like their homogeneity, becomes uncontrollable. Thus from the user side, two important points are to be called. The laser has to be chosen under consideration of requirements of the application. A further criterion is the machining duration. They amount to some 10 s for pulsed nitriding per square centimetre. By means of high-energy cw-treatments this time can be reduced on some seconds.

4.3 Transferability of the model system on arbitrary materials

From the investigations of the direct laser synthesis in reactive atmospheres at the model system TiN, many conclusions can be drawn, which seem to be independent of the material. Their validity still has to be verified. Using these conclusions it is possible to prepare an experiment under pre known conditions, in order to synthesize functional coatings efficiently. The following listing shows, what has to be essentially considered.

4.3.1 Evaporation temperature

The laser intensity should be chosen in such a way that the evaporation temperature is exceeded. However, it should not be too high in order to avoid the formation of a "key hole" or even to come into the range of the laser drilling treatments. If this condition is fulfilled, a plasma is induced, which finally leads to the shock wave and at least to dissociation in the surrounding background gas (here nitrogen). The resulting atomic nitrogen has a much higher adsorption capacity than the molecules (partial pressure/Sievert's law), so that efficient bounding of gas atoms onto the substrate follows.

4.3.2 Diffusion

It should be tried to melt as efficiently and deeply as possible. As the experiments and also different investigations showed, the diffusion coefficient, in particular for the reactive gas, is higher in the melts for orders of magnitude. From this behaviour it also results that the melting depth mainly determines the coating thickness.

4.3.3 Convection

Melt flow affects the synthesis result. These convective effects, like Marangoni-convection or also the melting ejection like the "Piston-effect", decrease rapidly the surface quality and lead to large coating in homogeneity. By means of the Prandtl-number Pr of a system it can be examined before the treatments, how strongly the convective behaviour will arise. As example a comparison between aluminium and titanium is demonstrated here. For Al a Pr of 0.012 is valid [125] and for titanium Pr = 0.11 is indicated. The knowledge of Pr offers the possibility to check the convective effects. Treatments on aluminium lead to much smaller convective effects like on titanium, thus nitriding of Al should result in better surface quality properties. Convection does not only have disadvantages, but offers even still another large advantage. It supports the diffusion process and even exceeds it. An efficient atom transport (here nitrogen) follows into deeper regions of the material. Schmidt-numbers SC of about 10, arising from simulations, prove this impressively.

4.3.4 Depth profile of the gas atoms

Like in particular simulations showed, the nitrogen profile determines the solidification direction. If close to the surface the gas atom concentration is high enough, the phases can be formed. This leads to a drastic change of the physical characteristics, in particular of the thermodynamics. Thus, the solidification starts from the surface into the depth like demonstrated in Sect. 3.4.

4.3.5 Solidification

The kind of the solidification morphology is determined by the lateral and longitudinal temperature gradients and the resulting cooling rates. In addition it is possible to reach a certain structure, if information about the velocity of the solidification front is available. This can be used, in order to minimize stress, to avoid cracks or also to maximize the hardness.

Drawing conclusions on the accomplished investigations it becomes clear that the FEL laser is an ideal tool for the coating synthesis, due to its many short intensive pulses. Most of the synthesis conditions are fulfilled. The pulse trains provide homogeneous plasma conditions above the substrate surface, which leads to a very efficient coating synthesis. The other commercial lasers have to be checked for their applicability. Of course attention must be paid on the choice of other materials and to other possible arising effects; however the represented processes are probably predominantly valid.

5 Summary

The accomplished experiments, analyzes, modelling and the discussed literature showed, which processes arise during the direct laser synthesis of functional coatings in reactive atmospheres using the model system titanium–nitrogen. The procedure offers an alternative to the conventional cladding techniques and particularly stands out

by its efficiency and the decrease of the process duration at moderate surface areas. The investigation of the procedure contains experiments at a free electron laser, at Nd:YAG lasers and at CO_2-, Excimer- and Ti:Sapphire lasers. As turned out, the physical processes taking place are very complex and closely coupled with each another, which is surprisingly due to the simple experimental structure. First it is important to know, which surface temperature is reached, because different process chains taking place. After that the process can be specified and controlled by estimation and suitable choice of laser intensities In the case of treatments above the evaporation threshold the process chain is most complex. Thus, the laser beam interaction time and the energy coupling are the first important parameters, followed by local heating and finally melting and evaporation. The thermodynamics of the entire system plays a crucial role, since material removal and plasma formation begin. This process results in the expansion of the ablated substrate atoms into the background gas, whereby this gets dissociated and ionized. This activation amplifies the adsorption on the material which gets treated and increases the synthesis efficiency. If the gas (here nitrogen) is inside the material, then transport processes arises. On the one hand naturally classical diffusion and in addition, convective mass transport, that is possible under certain conditions. Finally the solidification takes place, which determines the coating characteristics in particular the mechanical ones.

The evaluation of all results points out that it is possible to parameterize the direct laser synthesis. By means of an overlap-parameter and the pulse energy it is possible to define an empirical parameter which describes the energy entry per two dimensional surface elements. Correlations could be pointed out to microscopic and macroscopic coating properties like thickness and hardness. Regarding industrial and technical applicability, it is possible to synthesize custom-made coatings. According the investigations conclusions can be drawn in relation to treatments of other material combinations. This allows setting up general processing conditions for the direct laser synthesis. If possible the evaporation point should be exceeded, the melting depth should be maximized and convective effects should arise at moderate scales. They can be pre-estimated before an experiment, by the Prandtl-number of the system. Solidification morphologies are determined by temperature gradients and the velocity of solidification.

Again, the method offers an alternative to the techniques already established, as soon as certain special demands are made against the coatings. For wide area treatment this method does not represent a competitor to the long-proven ones. However, for specific applications like cutting tools etc. the procedure offers the possibility to synthesize to efficiently and sheep. The complexities of the processes taking place make it heavy to get accurate control of the method. This review show, which processes arise and how they have to be controlled.

Acknowledgments This work is supported by the Deutsche Forschungsgemeinschaft under grant DFG Scha 632/4. The Jefferson Lab is supported by the U.S. Dept. of Energy, the Office of Naval Research, the Commonwealth of Virginia and the Laser Processing Consortium. Kevin Jordan and Joseph F. Gubeli III are gratefully acknowledged for their assistance at the FEL. Prof. A. Emmel and Dr. R.Quietsch are gratefully acknowledged for their assistance during the Nd:YAG experiments. All contributors and involved researchers/technicians are acknowledged too.

References

1. Sproul WD (1996) Physical vapor deposition tool coatings. Surf Coat Technol 81:1–7
2. Crummenauer J (1995) TiN-Beschichtungen mittels Plasma-CVD. PhD thesis, Shaker Verlag, Aachen
3. Ritala M, Leskelä M, Rauhala E, Haussalo P (1995) Atomic layer epitaxy growth of TiN thin films. J Electrochem Soc 142:2731
4. Chowdhury R, Vispute RD, Jagannadham K, Narayan J (1996) Characteristic of titanium nitride films grown by pulsed laser deposition. J Mater Res 11:1458–1469
5. Baeuerle D (2000) Laser processing and chemistry, 3rd edn. Springer, New York
6. Kneubühl FK, Sigrist MW (1991) Laser. Teubner Verlag / GWV Verlag Fachverlage GmbH, Wiesbaden
7. Bloyce A, Morton PH, Bell T (1994) Surface engineering of titanium and titanium alloys (ASM International, Member/ Customer Service Center, Materials Park, OH 44073-0002, USA)
8. Weber H, Herziger G, Poprawe R (2004) Landolt-Börnstein numerical data and functional relationships in science and technology—laser physics and applications. Springer, Berlin
9. Steen WM (2003) Laser material processing. Springer, Berlin
10. Sun RL, Yang DZ, Guo LX, Dong SL (2001) Laser cladding of Ti-6Al-4V alloy with TiC and TiC+ NiCrBSi powders. Surf Coat Technol 135:307–312
11. Yunlian Q, Ju D, Quan H, Liying Z (2000) Electron beam welding, laser beam welding and gas tungsten arc welding of titanium sheet. Mater Sci Eng A 280:177–181
12. Basu S, DebRoy T (1992) Liquid metal expulsion during laser irradiation. J Appl Phys 72:3317
13. DebRoy T, David SA (1995) Physical processes in fusion welding. Rev Mod Phys 67:85–112
14. DebRoy T, Basu S, Mundra K (1991) Probing laser induced metal vaporization by gas dynamics and liquid pool transport phenomena. J Appl Phys 70:1313–1319
15. He X, Elmer JW, DebRoy T (2005) Heat transfer and fluid flow in laser microwelding. J Appl Phys 97:084909
16. Mishra S, DebRoy T (2005) A heat-transfer and fluid-flow-based model to obtain a specific weld geometry using various combinations of welding variables. J Appl Phys 98:044902
17. Schaaf P (2002) Laser nitriding of metals. Prog Mater Sci 47:1–161
18. Carpene E, Flank AM, Traverse A, Schaaf P (2002) EXAFS investigation of laser nitridation and laser carburization of silicon. J Phys D Appl Phys 35:1428–1432
19. Katsamas AI, Haidemenopoulos GN (2001) Laser-beam carburizing of low-alloy steels. Surf Coat Technol 139:183–191

20. Illgner C, Schaaf P, Lieb KP, Queitsch R, Barnikel J (1998) Material transport during excimer-laser nitriding of iron. J Appl Phys 83:2907
21. Sicard E, Boulmer-Leborgne C, Sauvage T (1998) Excimer laser induced surface nitriding of aluminium alloy. Appl Surf Sci 127:726–730
22. Katayama S, Matsunawa A, Morimoto A, Ishimoto S, Arata Y (1983) Laser Nitriding of Titanium and Its Alloys, Proc. 3rd Int. Colloq on Welding and Melting by Electron and Laser Beam, Lyon, France, p 219
23. Bergmann HW (1985) Thermochemische Behandlung von Titan und Titanlegierungen durch Laserumschmelzen und Gaslegieren. Materialwissenschaft und Werkstofftechnik 16:392–405
24. Ursu I, Mihailescu IN, Prokhorov AM, Konov VI, Tokarev VN, Uglov SA (1985) On the mechanism of surface compound formation by powerful microsecond pulsed TEA CO_2 laser irradiation in technical nitrogen. J Phys D Appl Phys 18:2547–2555
25. Walker A, Folkes JaS WM, West DRF (1985) Laser surface alloying of titanium substrates with carbon and nitrogen. Surface engineering 1:23–29
26. Bell T, Bergmann HW, Lanagan J, Morton PH, Staines AM (1986) Surface engineering of titanium with nitrogen. Surface engineering 2:133–143
27. Ayers JD (1984) Wear behavior of carbide-injected titanium and aluminum alloys. Wear 97:249–266
28. Ayers JD, Schaefer RJ, Robey WP (1981) A laser processing technique for improving the wear resistance of metals. J Metals 33:19
29. Hu C, Xin H, Watson LM, Baker TN (1997) Analysis of the phases developed by laser nitriding Ti-6Al-4V alloys. Acta Mater 45:4311–4322
30. Ignatiev M, Kovalev E, Melekhin I, Smurov IY, Sturlese S (1993) Hardening of a titanium alloy by laser nitriding. Wear 166:233–236
31. Morton PH, Bell (1988) T Surface engineering of titanium, Les editions de Physique, France pp 1705–1712
32. Morton PH, Bell T, Weisheit A, Kroll J, Mordike BL (1992) Laser gas nitriding of titanium and titanium alloys. In: Sudarshan TS, Braza JF (eds) Surface modification technologies V, Institute of Materials, 71st edn, pp 593–609
33. Mridha S, Baker TN (1991) Characteristic features of laser-nitrided surfaces of two titanium alloys. Mater Sci Eng A 142(1):115–124
34. Xin H, Mridha S, Baker TN (1996) The effect of laser surface nitriding with a spinning laser beam on the wear resistance of commercial purity titanium. J Mater Sci 31:22–30
35. Robinson JM, Anderson S, Knutsen RD, Reed RC (1995) Cavitation erosion of laser melted and laser nitrided Ti-6Al-4V. Mat Sci Technol-Lond 11:611
36. Bonss S, Brenner B, Beyer E (2001) Laser gas alloying of titanium—new possibilities for severe wear loaded components in medicine. Materialwissenschaft und Werkstofftechnik 32:160–165
37. Kloosterman AB, De Hosson JTM (1995) Microstructural characterization of laser nitrided titanium. Scripta Metallurgica et Materialia 33:567–573
38. Kloosterman AB (1998) Surface Modification of titanium with lasers. Groningen University Press, Groningen
39. Raaif M, El-Hossary FM, Negm NZ, Khalil SM, Kolitsch A, Höche D, Kaspar J, Mandl S, Schaaf P (2008) CO$_2$ laser nitriding of titanium. J Phys D Appl Phys 41:085208
40. Labudovic M, Kovacevic R, Kmecko I, Khan T, Blecic D, Blecic Z (1999) Mechanism of surface modification of the Ti-6Al-4V alloy using a gas tungsten arc heat source. Metall Mater Trans A 30:1597–1603
41. Nwobu AIP, Rawlings RD, West DRF (1999) Nitride formation in titanium based substrates during laser surface melting in nitrogen-argon atmospheres. Acta Mater 47:631–643
42. Xue L, Islam M, Koul AK, Bibby M, Wallace W (1997) Laser Gas Nitriding of Ti-6Al-4V Part 1: optimization of the Process. Adv Perform Mater 4:25–47
43. Labudovic M, Kovacevic R (2001) Modelling of the laser surface nitriding of Ti-6Al-4 V alloy: Analysis of heat transfer and residual stresses.Proceedings of the Institution of Mechanical Engineers, Part C. J Mech Eng Sci 215:315–340
44. Man HC, Zhao NQ, Cui ZD (2005) Surface morphology of a laser surface nitrided and etched Ti-6Al-4 V alloy. Surf Coat Technol 192:341–346
45. Golebiewski M, Kruzel G, Major R, Mroz W, Wierzchon T, Ebner R, Major B (2003) Morphology of titanium nitride produced using glow discharge nitriding, laser remelting and pulsed laser deposition. Mater Chem Phys 81:315–318
46. Man HC, Cui ZD, Yang XJ (2002) Analysis of laser gas nitrided titanium by X-ray photoelectron spectroscopy. Appl Surf Sci 199:293–302
47. Man HC, Cui ZD, Yue TM, Cheng FT (2003) Cavitation erosion behavior of laser gas nitrided Ti and Ti-6Al-4V alloy. Mat Sci Eng A 355:167–173
48. Mori JC, Serra P, Martianez E, Sardin G, Esteve J, Morenza JL (1999) Surface treatment of titanium by Nd:YAG laser irradiation in the presence of nitrogen. Appl Phys A: Mater Sci Process 69:699–702
49. Carpene E (2002) Excimer lasert treatments of iron, aluminium and silicon substrates in nitrogen and methane atmosheres. Universität Göttingen, Germany
50. Carpene E, Landry F, Schaaf P (2000) Modeling of nitrogen depth profiles in iron after nitriding with a homogenized laser beam. Appl Phys Lett 77:2412
51. Carpene E, Schaaf P, Han M, Lieb K, Shinn M (2002) Reactive surface processing by irradiation with excimer laser, Nd: YAG laser, free electron laser and Ti: sapphire laser in nitrogen atmosphere. Appl Surf Sci 186:195–199
52. Carpene E, Shinn M, Schaaf P (2005) Synthesis of highly oriented TiN_x coatings by free-electron laser processing of titanium in nitrogen gas. Appl Phys A: Mater Sci Process 80:1707–1710
53. Carpene E, Shinn M, Schaaf P (2005) Free-electron laser surface processing of titanium in nitrogen atmosphere. Appl Surf Sci 247:307–312
54. Höche D, Müller S, Shinn M, Rapin G, Remdt E, Gubisch M, Schaaf P (2009) Marangoni convection during free electron laser nitriding of titanium. Metall Mater Trans B 40 497507
55. Höche D, Rapin G, Kaspar J, Shinn M, Schaaf P (2007) Free electron laser nitriding of metals: From basis physics to industrial applications. Appl Surf Sci 253:8041–8044
56. Höche D, Rapin G, Schaaf P (2007) FEM simulation of the laser plasma interaction during laser nitriding of titanium. Appl Surf Sci 254:888–892
57. Höche D, Schikora H, Zutz H, Emmel A, Queitsch R, Schaaf P (2008) TiN-coating formation by pulsed Nd: YAG laser irradiation of titanium in nitrogen. J Coat Technol Res 5:505–512
58. Höche D, Schikora HaZ H, Queitsch R, Emmel AaS P (2008) Microstructure of TiN coatings synthesized by direct pulsed Nd: YAG laser nitriding of titanium: development of grain size, microstrain, and grain orientation. Appl Phys A: Mater Sci Process 91:305–314
59. Höche D, Shinn M, Kaspar J, Rapin G, Schaaf P (2007) Laser pulse structure dependent texture of FEL synthesized TiN_x coatings. J Phys D Appl Phys 40:818–825
60. Höche D, Shinn M, Müller S, Schaaf P (2009) Diffusion, convection, and solidification in cw-mode free electron laser nitrided titanium. J Appl Phys 105:083503–083506

61. Schaaf P (2003) Laser nitriding and laser carburizing of surfacesALT'02 International Conference on Advanced Laser Technologies, 1 edn SPIE, pp 404–415
62. Schaaf P, Han M, Lieb KP, Carpene E (2002) Laser nitriding of iron with laser pulses from femtosecond to nanosecond pulse duration. Appl Phys Lett 80:1091–1093
63. Schaaf P, Landry F, Lieb KP (1999) Origin of nitrogen depth profiles after laser nitriding of iron. Appl Phys Lett 74:153–155
64. Carpene E, Schaaf P (2002) Mass transport mechanisms during excimer laser nitriding of aluminum. Phys Rev B 65:224111
65. Schaaf P, Landry F, Neubauer M, Lieb KP (1998) Laser nitriding investigated with Mössbauer spectroscopy. Hyperfine Interact 113:429–434
66. Han M, Lieb KP, Carpene E, Schaaf P (2003) Laser–plume dynamics during excimer laser nitriding of iron. J Appl Phys 93:5742–5749
67. Han M (2001) Laser nitriding of metals. Georg-August Universität, Göttingen
68. Chichkov BN, Momma C, Nolte S, von Alvensleben F, Tünnermann A (1996) Femtosecond, picosecond and nanosecond laser ablation of solids. Appl Phys A: Mater Sci Process 63:109–115
69. Anisimov SI, Kapeliovich BL, Perel'Man TL (1974) Electron emission from metal surfaces exposed to ultrashort laser pulses. Soviet Phys JETP 39:375
70. Wu JD, Wu CZ, Zhong XX, Song ZM, Li FM (1997) Surface nitridation of transition metals by pulsed laser irradiation in gaseous nitrogen. Surf Coat Technol 96:330–336
71. Trtica M, Gakovic B, Batani D, Desai T, Panjan P, Radak B (2006) Surface modifications of a titanium implant by a picosecond Nd:YAG laser operating at 1064 and 532 nm. Appl Surf Sci 253:2551–2556
72. Santos EC, Morita M, Shiomi M, Osakada K, Takahashi M (2006) Laser gas nitriding of pure titanium using CW and pulsed Nd:YAG lasers. Surf Coat Technol 201:1635–1642
73. Ettaqi S, Hays V, Hantzpergue JJ, Saindrenan G, Remy JC (1997) Mechanical, structural and tribological properties of titanium nitrided by a pulsed laser. Surf Coat Technol (Switzerland) 100:428–432
74. Gyorgy E, Perez del Pino A, Serra P, Morenza JL (2002) Surface nitridation of titanium by pulsed Nd:YAG laser irradiation. Appl Surf Sci 186:130–134. doi:10.1016/S0257-8972(03)00520-6
75. Gyorgy E, Perez del Pino A, Serra P, Morenza JL (2003) Depth profiling characterisation of the surface layer obtained by pulsed Nd:Yag laser irradiation of titanium in nitrogen. Surf Coat Technol 173:265–270
76. Xue L, Islam M, Koul AK, Bibby M, Wallace W (1997) Laser gas nitriding of Ti-6Al-4V Part 2: characteristics of nitrided layers. Adv Perform Mater 4:389–408
77. Gazanion F, Tremblay R, Fiset M, Dube D (2003) Improvement of abrasive wear resistance of titanium by laser gas alloying in nitrogen-air atmosphere. Can Metall Q 42:235–244
78. Gyorgy E, Perez del Pino A, Serra P, Morenza JL (2003) Microcolumn development on titanium by multipulse laser irradiation in nitrogen. J Mater Res 18:2228–2234
79. Gyorgy E, Perez del Pino A, Serra P, Morenza JL (2005) Laser-induced growth of titanium nitride microcolumns on biased titanium targets. J Mater Res 20:62–67
80. Covelli L, Pierdominici F, Smurov I, Tosto S (1996) Surface microstructure of titanium irradiated by Nd: YAG pulsed laser in presence of carbon and nitrogen. Surf Coat Technol (Switzerland) 78:196–204
81. Yu HJ, Sun FJ, Zhang J (2009) Laser and plasma nitriding of titanium using CW-CO2 laser in the atmosphere. Curr Appl Phys 9:227–233. doi:10.1016/j.cap.2008.01.013
82. Garcia I, De Damborenea JJ (1998) Corrosion properties of TiN prepared by laser gas alloying of Ti and Ti6Al4V. Corros Sci 40:1411–1419
83. Abboud JH, Fidel AF, Benyounis KY (2008) Surface nitriding of Ti-6Al-4V alloy with a high power CO2 laser. Opt Laser Technol 40:405–414
84. Hu C, Baker TN (1999) A semi-empirical model to predict the melt depth developed in overlapping laser tracks on a Ti-6Al-4V alloy. J Mater Process Technol 94:116–122
85. Xin H, Watson LM, Baker TN (1998) Surface analytical studies of a laser nitrided Ti-6Al-4V alloy: a comparison of spinning and stationary laser beam modes. Acta Mater 46:1949–1961
86. Baker TN, Selamat MS (2008) Surface engineering of Ti6Al4V by nitriding and powder alloying using CW CO2 laser. Mater Sci Technol 24:189–200
87. Thomann AL, Boulmer-Leborgne C, Andreazza-Vignolle C, Andreazza P, Hermann J, Blondiaux G (1996) Metal surface nitriding by laser induced plasma. J Appl Phys 80:4673
88. Yilbas BS, Karatas C, Keles O, Usta IY, Ahsan M (2006) CO_2 laser gas assisted nitriding of Ti–6Al–4V alloy. Appl Surf Sci 252:8557–8564
89. Xin H, Hu C, Baker TN (2000) Microstructural assessment of laser nitrided Ti-6Al-4V alloy. J Mater Sci 35:3373–3382
90. Mridha S, Baker TN (1994) Crack-free hard surfaces produced by laser nitriding of commercial purity titanium. Mater Sci Eng A 188:229–239
91. Mridha S, Baker TN (1991) Characteristic features of laser-nitrided surfaces of two titanium alloys. Mater Sci Eng A 142:115–124
92. Kaspar J, Luft A, Bonß S, Winderlich B, Brenner B (2002) Mikrostrukturelle Charakterisierung eigenschaftsdegradierender Mechanismen während der Schnellerwärmung und–abkühlung beim Lasergaslegieren von Titanwerkstoffen. In: G. S (ed) Kurzzeitmetallurgie Handbuch zum Abschlußkolloquium des DFG-Schwerpunkts Bremen: BIAS, 2002 (Strahltechnik 18) DFG, Bremen, pp 153–162
93. Kaspar J, Bretschneider J, Jacob S, Bonsharp S, Winderlich B, Brenner B (2007) Microstructure, hardness and cavitation erosion behaviour of Ti6Al4V laser nitrided under different gas atmospheres. Surf Eng 23:99–106
94. L'Enfant H, Laurens P, St Catherine MC, Dubois T, Amouroux J (1997) Kinetics of titanium nitriding under CW CO2 laser radiation. Surf Coat Technol 96:169–175
95. Liu JL, Luo QQ, Zou ZR (1993) Laser gas alloying of titanium-alloy with nitrogen. Surf Coat Technol 57:191–195
96. Bonss S, Brenner B, Scheibe HJ, Ziegele H (1997) Laser gas alloying—manufacturing process for wear resistant layers on titanium alloys. Materialwissenschaft und Werkstofftechnik 28:524–528
97. Weerasinghe VM, West DRF, deDamborenea J (1996) Laser surface nitriding of titanium and a titanium alloy. J Mater Process Technol 58:79–86
98. Zimnicki J, Rozniakowski K, Wendler B, Kalita W, Hoffman J (1998) Creation of TiN paths on titanium alloy OT4–1 by the use of a laser beam. J Mater Sci 33:1385–1388
99. Hu C, Baker TN (1999) The importance of preheat before laser nitriding a Ti-6Al-4 V alloy. Mater Sci Eng A Struct Mater 265:268–275
100. Hu C, Baker T (1997) Overlapping laser tracks to produce a continuous nitrided layer in Ti–6Al–4V alloy. J Mater Sci 32:2821–2826
101. Raaif M, El-Hossary FM, Negm NZ, Khalil SM, Kolitsch A, Hoeche D, Kaspar J, Maendl S, Schaaf P (2008) CO2 laser nitriding of titanium. J Phys D-Appl Phys 41:085208

102. Laurens P, LEnfant H, SainteCatherine MC, Blechet JJ, Amouroux J (1997) Nitriding of titanium under CW CO2 laser radiation. Thin Solid Films 293:220–226
103. Thomann AL, Sicard E, Boulmer-Leborgne C, Vivien C, Hermann J, Andreazza-Vignolle C, Andreazza P, Meneau C (1997) Surface nitriding of titanium and aluminium by laser-induced plasma. Surf Coat Technol 97:448–452
104. D'Anna E, Leggieri G, Luches A, Martino M, Perrone A, Mengucci P, Mihailescu IN (1992) Multilayer titanium nitride and silicide structures synthesized by multipulse excimer laser irradiation. Appl Surf Sci 54:353–357
105. D'Anna E, Leggieri G, Luches A, Martino M, Drigo AV, Mihailescu IN, Ganatsios S (1991) Synthesis of pure titanium nitride layers by multipulse excimer laser irradiation of titanium foils in a nitrogen-containing atmosphere. J Appl Phys 69:1687
106. Yue TM, Yu JK, Mei Z, Man HC (2002) Excimer laser surface treatment of Ti–6Al–4V alloy for corrosion resistance enhancement. Mater Lett 52:206–212
107. Mihailescu I, Chitica N, Nistor L, Popescu M, Teodorescu V, Ursu I, Andrei A, Barborica A, Luches A, De Giorgi M (1993) Deposition of high quality TiN films by excimer laser ablation in reactive gas. J Appl Phys 74:5781
108. Mihailescu I, Chitica N, Teodorescu V, De Giorgi M, Leggieri G, Luches A, Martino M, Perrone A, Dubreuil B (1993) Excimer laser reactive ablation: an efficient approach for the deposition of high quality TiN films. J Vac Sci Technol A 11:2577
109. Mihailescu I, Gyorgy E, Chitica N, Teodorescu V, Mavin G, Luches A, Perrone A, Martino M, Neamtu J (1996) A parametric study of the deposition of the TiN thin films by laser reactive ablation of titanium targets in nitrogen: the roles of the total gas pressure and the contaminations with oxides. J Mater Sci 31:2909–2915
110. Bendavid A, Martin PJ, Netterfield RP, Kinder TJ (1996) Characterization of the optical properties and composition of TiN_x thin films by spectroscopic ellipsometry and X-ray photoelectron spectroscopy. Surf Interface Anal 24:627–633
111. Niyomsoan S, Grant W, Olson DL, Mishra B (2002) Variation of color in titanium and zirconium nitride decorative thin films. Thin Solid Films 415:187–194
112. Jonsson B, Hogmark S (1984) Hardness measurements of thin films. Thin Solid Films 114:257–269
113. Shuja SZ, Yilbas BS, Budair MO (1998) Modeling of laser heating of solid substance including assisting gas impingement. Numer Heat Transf A:Appl 33:315–339
114. Lengauer W (1992) Properties of bulk-TiN_{1-x} prepared by nitrogen diffusion into titanium metal. J Alloys Compd 186:293–307
115. Nagakura S, Kusunoki T, Kakimoto F, Hirotsu Y (1975) Lattice parameter of the non-stoichiometric compound TiN_x. J Appl Crystallogr 8:65–66
116. Neamtu J, Mihailescu IN, Ristoscu C, Hermann J (1999) Theoretical modelling of phenomena in the pulsed-laser deposition process: Application to Ti targets ablation in low-pressure N_2. J Appl Phys 86:6096–6106
117. Wood FW, Paasche OG (1977) Dubious details of nitrogen diffusion in nitrided titanium. Thin Solid Films 40:131–137
118. Benson S, Biallas G, Boyce J, Bullard D, Coleman J, Douglas D, Dylla F, Evans R, Evtushenko P, Grippo A (2007) The 4th generation light source at Jefferson Lab. Nuclear Inst Methods Phys Res A 582:14–17
119. Shinn MD (2000) High-average-power free-electron lasers: a new laser source for materials processing. Proceedings of SPIE 4065:434–440
120. Fisher K, Kurz W (1986) Fundamentals of Solidification. Trans. Tech. Publications Co., Switzerland
121. Mohanty PS, Mazumder J (1998) Solidification behavior and microstructural evolution during laser beam - material interaction. Metall Mater Trans B 29:1269–1279
122. Zhou J, Tsai HL, Wang PC (2006) Transport phenomena and keyhole dynamics during pulsed laser welding. J Heat Transf 128:680–690
123. Kurz W, Bezençon C, Gäumann M (2001) Columnar to equiaxed transition in solidification processing. Sci Technol Adv Mater 2:185–191
124. Lu SZ, Hunt JD (1992) A numerical analysis of dendritic and cellular array growth: the spacing adjustment mechanisms. J Cryst Growth 123:17–34
125. Robert A, Debroy T (2001) Geometry of laser spot welds from dimensionless numbers. Metall Mater Trans B 32:941–947